FINITE DEFORMATION OF INTERNALLY PRESSURIZED COMPRESSIBLE SYNTHETIC RUBBER-LIKE MATERIAL

BY

EGBUHUZOR, UDECHUKWU PETER

(B.Sc, Mathematics; M.Sc, Applied Mathematics)

REGISTRATION NUMBER:20134877928

A DISSERTATION SUBMITTED TO THE POSTGRADUATE SCHOOL, FEDERAL UNIVERSITY OF TECHNOLOGY, OWERRI, NIGERIA.

IN PARTIAL FULFILLMENT OF THE REQUIREMENTS FOR THE AWARD OF THE DOCTOR OF PHILOSOPHY(Ph.D.) DEGREE IN MATHEMATICS

JULY, 2021

CERTIFICATION

This is to certify that the work "FINITE DEFORMATION OF INTERNALLY PRESSU
IZED COMPRESSIBLE SYNTHETIC RUBBER-LIKE MATERIAL", was carried out
EGBUHUZOR, UDECHUKWU PETER (20134877928) in partial fulfillment of the requi
ments for the award of the Degree of Doctor of Philosophy of Science (Ph.D.) in Mathematics
the Department of Mathematics, Federal University of Technology, Owerri.

PROF. E.N. ERUMAKA
(PRINCIPAL SUPERVISOR) — DATE 06/09/21

PROF. A.M. ETTE
(CO - SUPERVISOR) — DATE 08/09/2021

DR.(MRS.) E. E. ONUGHA
(CO - SUPERVISOR) — DATE 06/09/2021

PROF. E. N. ERUMAKA
(HEAD OF DEPARTMENT) — DATE 06/09/21

PROF. C. C. Z. AKAOLISA
(DEAN, SCHOOL OF PHYSICAL SCIENCES) — DATE 27/9/2021

PROF. C. C. EZE
(DEAN, SCHOOL OF POST GRADUATE STUDIES) — DATE

PROF. JAMES N NNADI
(EXTERNAL EXAMINER) — DATE 26/7/21

DEDICATION

This work is dedicated to God Almighty.

ACKNOWLEDGEMENTS

My heartfelt gratitude goes to God almighty for the journey so far. I also express my love for our mother Mary who interceded while on this program. I thank my supervisors, Prof. E.N. Erumaka who is always humble and ready to assist at all time, Prof. A.M.Ette and Dr. E. E. Onugha for their constructive criticisms and advice. I thank Dr. Obi Martins our Departmental Postgraduate coordinator for his advice, constructive criticisms and directives. I sincerely appreciate the erudite scholars and lecturers of this Department such as Prof. S.C. Inyama, Prof. I. Iwueze, Dr. Nse Celestine, Dr. Chukwuchekwa Joy, Dr. Andrew Omame and all the lecturers in Mathematics department who helped to better this work by their meaningful contributions. My thanksgiving goes to My mentors Mr. Uwazie Luke, Prof. Stephane Bordas and Prof. Nkem Ogbonna whose support and love built my confidence to study Mathematics to this level. I recognize the efforts of Dr. Modobei Ifeanyi for his contributions during the analysis.

To my wonderful wife, my love for her remains unrivalled and I can not thank her enough for her support. In a special way, I wish to appreciate my little angels(Chukwunyere Chiziterem, Chukwunyere Chiedozie and Chukwunyere Chigozie) whose prayers kept me pushing so hard for success. I thank my parents(Sir & Lady B.C. Egbuhuzor), my Parents-inlaw(Chief & Lolo Dominic Ewuchie), my brother(Egbuhuzor Chidume), my brother-inlaw(Ewuchie Chinedu) and my sisters(Egbuhuzor Nyeaka, Egbuhuzor Chimma and Egbuhuzor Akuchi) and my entire relatives. Finally, my special

gratitude goes to my Dr. Franca Okumor, Dr. Chilaka Francis, Dr.Raimi Lasisi, Nwanneka Amoge, Mezie Enyinnaya,Daniel Awomukwu and many others for their importantant contributions towards the success of this work.

Contents

List of Figures

List of Tables

ABSTRACT

The finite deformation of internally pressurized isotropic compressible synthetic rubber material governed by Levinson and Burgess strain energy function is analysed. The analysis led to a second-order nonlinear ordinary differential equation for the determination of stresses and displacements. Analytic solution is found impossible for now, hence, the solution is sought numerically using two methods namely shooting method and collocation method on mathematica(ode45 solver). The simulation of the system is made for $\rho = 14N/m^2$, and the cylindrical symmetric deformation attained its maximum displacements and stresses at $r(1) = 1.16638m$ and $\sigma_{rr} = (-1.2973e - 05)kg/m/s^2$ while at $\rho = 0.5N/m^2$, the spherical symmetric deformation obtained its maximum displacements and stresses at $r(1) = 0.01853m$ and $\sigma_{rr} = (-0.00035)kg/m/s^2$ respectively. The results of the two schemes were statistically compared using t-test and results obtained showed, the two methods have no significant difference. Similarly, for the cylindrical deformation, the t-test showed that the two methods have no significant difference which validates the solutions.

Keywords: Deformation, stresses, Displacements, collocation, shooting method and rubber-like

Chapter 1

INTRODUCTION

1.1 BACKGROUND OF STUDY

Elasticity in general mathematical physics is the ability of a body to regain its original shape or size when a distorting force is removed. The theory of materials subjected to and survive large deformations is basically nonlinear and nonlinear materials have been found to be more realistic in practical terms, especially in engineering field and construction firms. The nature of mathematical models in theory of elasticity make the derived equations very tough and sometimes impossible to obtain analytical or closed form solution to the problem. Our choice of hollow sphere and cylinder is not a new choice. In the works of Chen and Durelli(1974), Huang(1985), Stange(1984) and Hill(1993) In the modeling of any hyper-elastic material, the major focus is on selecting the proper constitutive relation. Here we consider the hyper-elastic material to be a rubber material. Rivlin(1949), Green and Zerna(1968), Ogden, Chadwick and Haddon(1973) and Ogden(2001) assumed $r = R$, where the r is the deformed configuration and R is the undeformed configuration of the hollow cylinder. They considered the strain energy function of Ogden material for their work.Our work is an extension of the work carried out by Levinson and Burgess(1971). They were able to obtain the different

behaviours of the polynomial materials and compared it with different other strain energy functions. Rubber is not just about the original natural rubber but also referred to any material that has same mechanical properties and they are in other words said to be rubber-like materials.

In our work, we will concentrate on synthetic rubber which is made from petroleum and it is grouped as an artificial rubber. The synthetic rubber can be deformed without being damaged and the original shape is preserved after being stretched. This type of rubber is man-made and has much importance over natural rubber due to its superiority in performance. It is used often than natural rubber in most industrialized nations especially in producing car tyres, medical equipment, machinery belts, moulded parts and synthetic rubbers are said to be elastomers. The material is said to be Isotropic since the assumed body have same properties in all directions. Rubbers, metals, concrete, etc are few examples of isotropic materials. Many material solids have similar properties all through their volumes. The material considered here is independent of the spatial coordinates and it is called homogeneity while the material property is a homogeneous material.

Kumar and Rao(2016) discussed hyperelastic rubber-like material considering different strain energy functions, specifically, neo-Hookean, Mooney-Rivlin, Ogden and Yeoh Homogeneity guarantees uniformity of the body. This homogeneity assumption is valid as long as it depends on the volume of the body. Our choice of material is based on the fact that a lot has been achieved on natural rubbers but not much has been achieved in synthetic rubber materials due to the difficult nature of its model equations.

Many researchers and authors have worked on elastic materials and their deformations when under internal and external forces. Deformation is the tendency of a solid material to assume its original shape after being acted upon by an applied force. Once the force is removed, the object will return

to its original shape or size as long as the material is elastic. When the curve of the load between stress and strain is linear, then the material is said to be linearly elastic but if the curve between curve of the load between stress and strain is nonlinear, the material is said to be a nonlinearly elastic material. Every rubber or rubber-like material is said to be nonlinearly elastic. In elastic materials, loading is easily reversible and there is temporary deformation. No energy is lost and deformation happens immediately and does not depend on how the strain or stress is obtained. Moreover, the elastic behaviour does not depend on time.There are two basic ways to understand the physical behaviour of certain materials; we have the physical and phenomenological approach. A physical approach is when a body is assumed to consist of atoms, molecules and crystals. The behaviour of the body is based on the interaction with these atoms and molecules. It is very difficult to apply this physical approach to engineering structures, especially in buildings and air crafts even though this approach gives a very clear idea of deformable bodies. Deformation is the disorientation or distortion of material elements from its original position called undeformed configuration, usually as a result of application of external forces on the body. Deformation in a material can last only for a short while and it reverses itself after the removal of the applied force, so that the body assumes its original shape. In other words, deformation can result to a change in size or shape or possibly both.There are two types of material modes and we shall consider Material or Lagrangian mode which is the point that deals with the object of our study considering the motion and deformation of the body, the material point or mode takes up different spatial modes in space. You just need to fix a volume in space and identifying a spatial mode will be very simple. This can be expressed by the mapping; $x = x(X)$. The Spatial or Eulerian mode is the mode fixed in space. Individual material bodies can take up the same spatial point at separate

instants of time. This can be expressed mathematically as $X = X(x)$. Here, we use the phenomenological approach which treats problems by the constructs of mathematical frame work. For a rubber-like material, compressibility is an important physical property constantly needed in practical applications and in calculations that relates to mechanical properties. This is because rubber-like materials exhibit a highly nonlinear behaviour and can be applied to rubber and many other polymeric materials which are considered to be isotropic and hyper-elastic material. We are most concerned about the deformations of Levinson-Burgess proposed strain energy function which is said to be compressed. Going through this work, in the literature review, we are provided with an insight of work done in this area of elasticity. Different works done by different authors were explained in the form, conceptual literature, related literature and specific literature where we highlighted our main target to achieve at the end of this work.

The methodology led us into using the necessary tools to develop the governing equations for the spherical and cylindrical symmetric deformations of internally pressurized hollow sphere and hollow cylinder respectively. This process shall take us through determining the deformation gradient tensor. The deformation Gradient Tensor (F), can be expressed in component form as: $F_{iR} = \frac{\partial x_i}{\partial X_R}$, the principal invariants, the Cauchy green tensor can be expressed as left and right Cauchy-Green strain tensors and it gives a measure of how the lengths of line elements and angles between line elements change between configurations. It determines how much the line segment stretches. We determined the Cauchy stresses and finally, we obtained a boundary value model equation which we solved in chapter four of this work by comparing shooting method and collocation method. A statistical analysis using t-test was implemented to determine which method is better in the solution of the nonlinear second-order ordinary differential equation and we wrote

codes on mathematica (ode45 solver) for both method to ascertain the stresses and displacement of the rubber material undergoing internal pressure due to inflation. Finally, in chapter five, we made our conclusions and recommendations from the analysis of results obtained. References to journals and textbooks will be adequately provided throughout the thesis in the prescribed form by the University standard.

The strain energy function, W, as proposed by Levison and Burgess(1971) is given as:

$$W = \frac{\mu_0}{2}\left[f(J_1 - 3) + (1-f)(J_2 - 3) + 2(1-2f)(J_3 - 1) + 2f + \frac{4v-1}{1-2v}(J_3 - 1)^2\right] \quad (1.1)$$

where $J_1 = I_1 = {\lambda_1}^2 + {\lambda_2}^2 + {\lambda_3}^2$, $J_2 = \frac{I_2}{I_3} = \frac{1}{{\lambda_1}^2} + \frac{1}{{\lambda_2}^2} + \frac{1}{{\lambda_3}^2}$ and

$J_3 = \sqrt{I_3} = \sqrt{{\lambda_1}^2{\lambda_2}^2{\lambda_3}^2} = \lambda_1\lambda_2\lambda_3$

I_1, I_2 and I_3 are the principal invariants of the Cauchy-Green stress tensor while λ_1,λ_2,λ_3 are the eigenvalues.

f and v are the material constants and poisson ratio respectively while μ_0 is the ground state shear modulus.

Levinson and Burgess(1971), showed in an experimental result that for highly compressible polyurethane foam rubber, $f = 0$ and $v = 0.25$ will reduce equation(1.1) to Blatz-Ko generalized strain energy function.

If $f = 0$ and $v = 0.5$, equation(1.1) reduces to the Neo-Hookean strain energy function. Similarly, Mooney-Rivlin material for incompressible material will be obtained as $I_3 = 1$ when $f = 1$ and $v = 0.5$.

1.1.1 PROBLEM STATEMENT

The failure of cylindrical and spherical bodies undergoing internal pressure has been on the increase.Research works are on the increase on how best to determine the different behaviour of such materials. This research work is set to determine the behaviour of such bodies governed by the strain energy functions proposed by Levinson-Burgess under internal pressure. This is mainly because this model governs bodies composed of synthetic rubber.

1.1.2 OBJECTIVES OF STUDY

- The main objective of this work is to determine the stresses and displacements in a typical spherical and cylindrical compressible, symmetric, synthetic, rubber-like materials deforming under internal pressure.

Specific objectives are as follows:

- To adopt the field equation of finite elasticity to the synthetic rubber-like material and determine the appropriate boundary conditions.
- To use Mathematica (ode45 solver) software and collocation method to solve the resulting nonlinear second-order ordinary differential equation
- To determine the maximum displacements and stresses at a certain pressure for both the spherical and cylindrical material deformations and comparing our result from the ode45 solver with the collocation method on mathematica software.
- To use statistical analysis(t-test) to examine if there is a significant difference in the results obtained in the methods of solutions for both spherical and cylindrical deformations.

1.1.3 JUSTIFICATION OF STUDY

The Neo-Hookean model which is one of the simplest and widely used strain energy function is normally used to predict the behaviour of incompressible rubber-like material but our choice of using this material is because the strain energy function is in a generalized form and it reduces to different strain energy functions when certain conditions are considered. It can be applied to predict both the compressible and incompressible deformation of rubber-like materials. Moreover, we are yet to see other literature apply this strain energy function by Levinson and Burgess in solving the stresses and displacements of synthetic rubber using same method as applied in our work.

1.1.4 SCOPE OF STUDY

This work is limited to isotropic hyper-elastic compressible synthetic material of a Levinson & Burgess strain energy function. However, the frame work can accommodate other strain energy functions and the resulting model equations may be solved by same method.

Chapter 2

LITERATURE REVIEW

2.1 CONCEPTUAL LITERATURE

We are to consider the general theory of materials subjected to large deformations which are nonlinear. Nonlinear materials have been discovered to be more realistic in practical terms, especially in engineering fields and construction firms. When modeling a hyper-elastic material, the major focus is on selecting the proper constitutive relations. Poligne and Horgan (1991) studied a special case for some large deformations of homogeneous isotropic compressible nonlinearly elastic solids.A two-point boundary value problem of second order nonlinear ordinary differential equation was derived. For such materials other than the incompressible case, volume change is inevitable. The resulting boundary value problems are generally difficult to obtain analytically for compressible materials than that of incompressible materials. The problem solved by Polignone and Horgan (1991) is to determine deformations of a class of isochoric compressible materials. The research work carried out by Kanner and Horgan(2008) on extension and torsion of strain-stiffening discussed the effect on the response of soild circular cylinders in the combined deformation of torsion layered on axial extension. The result of axial force required to maintain

pure torsion is compressive for the models considered. The results they ascertained are totally different and opposite with those obtained for other models such as Mooney-Rivlin and neo-Hookean. Ericksen (1955) explained that deformation cannot be universai. There are a number deformations which can replicate in every incompressible, isotropic, perfectly elastic material under surface traction. Solutions corresponding to the these deformations are said to be rubber. According to Kao, Steven, Kendall, Kurt, Stenmark, and Jerryl(2009), Most of the starting point for modeling of various kinds of elastomers is the strain energy function. They discussed the deformation of fibre materials composed of soft matrix which is re-inforced with stiffer fibres.The material considered is said to be an isotropic neo-Hookean material. Anisotropic behaviour was introduced by adding a structure tensor characterizing the valid orientation distribution of the stress-strain behaviours of the fibre.They also developed stress-stretch response of the model under uniaxial loading. Peyrant, Feng, and He(2009) derived the tangent operator and stress tensor by applying Finite Element Method(FEM) in their study of deformations of hyperelastic model. Three test sample including homogeneous and non-homogeneous deformation are proposed to demonstrate the formulated model. The paper used Ogden's hyperelastic model in modeling the finite deformation of the bodies. In the results, three test examples were performed which include homogeneous and non-homogeneous deformations to validate the deveoped algorithms. Ali, Hosseini, and Sahari(2010) in their work on A review and comparison on some rubber elasticity models in reviewed different classical continuum mechanics models for incompressible and isotropic materials dependent on strain energy potential which compares to neo-Hookean, Yeoh, Mooney-Rivlin and Ogden models in predicting uniaxial deformation. ABAQUS and material curve fitting was applied for neo-Hookean(Reduced Polynomial form with N=1), Yeoh(Reduced

polynomial form with N=3), Mooney-Rivlin(Polynomial form with N=1) and Ogden with N= 1. Fitting for Ogden and Yeoh models for small and large strain responses was shown to be better than that of Mooney-Rivlin and neo-Hookean when calibrated with uniaxial data. The model contains a deformation mode-independent properties and the work by Hoss(2010) on a new constitutive model for rubber-like materials reviews the different strain energy functions for several constitutive models focusing on incompressible elsatomers. They proposed a new family of hyperelastic models and the strain energy functions retains both terms of the stiffening and that representing the characteristic oscillation in the stress vs strain curve undergoing small strains. Volokh(2010) explained that strain energy increases ultimately with increase of deformation. He introduced failure in hyperelasticity by replacing the strain energy of an intact material with a modified one. This new strain energy was use to model failure of natural rubbers(NR) and styrene-butadiene(SBR) rubbers under plane stress conditions to the available experiments and other theories. The study by Jongmin and Dirk(2011) specifically outlined the experiments carried out at different strain rates on continuous loading and unloading to characterize the deformation behaviour of polyurea under compressive loading. They developed td a new model which predicts the response under monotonic loading given wide range of strain rates and the result agreed well with the experimental result. Akhundov and Skripochka(2011) discovered that the cylindrical deformations can be described using model of plane deformations. The deformation of cylinders with sliding and rigid fits on their inner surface was considered in free rotation. They discovered that the deformation of the cylinders can be described by means of the model of plane deformation. Hossain and Steinman(2012) used phenomenological and micromechanical motivated network models for nearly incompressible hyperelastic polymeric materials in their paper on More

hyperelastic models for rubber-like materials: consistent tangent operators and comparative study. They applied finite element framework for the solution of boundary value problem as derived in their work. In their result, they obtained and analyzed three homogeneous deformation modes which includes uniaxial tension, equibiaxial tension and pure share. The work of Horgan and Murphy(2012) in their paper on finite extension and torsion of fibre-re-inforced non-linearly elastic circular cylinders, considered a class of incompressible anisotropic materials withstrain energy densities which is in logarithm form in the anisotropic invariants. The anisotropy led to a larger mechanical response than was found for isotropic strain-stiffening materials. These models has limited fibre extensibility which is stretch induced strain stiffening of collagen fibres on loading. The obtained results impacted more on extension-torsion tests for fibre reinforced fibre. Akhundov and Lunev(2013) improved on his earlier work by solving the problem of tyre. The model made use of applied theory of vibrous material with small and large strains.

Some other authors introduced many other approach to solving the problems of hyperelastic models. Fereidoonnezhad, Naghdabadi, and Arghavanil(2013) instead of applying failure, rather used their proposed strain energy function to characterize the behaviour of a tranversely isotropic incompressible fibre reinforced rubber. The result of their prediction agreed with the experimental data for both tensile and shear deformations. Moreira, and Numesl(2013) compared two types of deformation using experimental and theoritical methods. Result showed that simple shear cannot be considered as pure shear combined with a rotation when undergoing large deformation. It is a fact that rubber-like materials undergo large deformation and nonlinearly upon loading and they return to the initial configuration after the removal of load. Khajehasaeid, Arghavani, and Naghdabadi(2013) developed a strain energy function for incompressible isotropic rubbers which

satisfies all properties of hyperelastic model. The proposed strain energy function was compared to that of Mooney–Rivlin, Pucci–Saccomandi models and Treloar's uniaxial extension data. The proposed model comforms very much with the existing models. Extensively, Akhundov(2014) presented the results discovered in modeling large deformations of fibrous bodies of revolution based on applied and carcass theories. fibre-reinforced bodies under large deformation was obtained by the help of single-level applied and two-level carcass theories. The body was investigated by the applied theory at a high fibre content. This was also similar to the paper by Pence and Gou(2015) considered three different compressible versions of the conventional incompressible neo-Hookean material model. The three versions critically considered the differences with respect to each other by use of neo-Hookean strain energy function. Their aim is to exhibit these differences which their work effectively addressed.

Horgan(2015) also reviewed some of the numerous developments, extensions and widespread application resulting from not just this paper but papers in rubber elasticity and even biomechanics of soft biomaterials. They developed a simple but emprical mathematical model whcih is strain stiffening at large strains during their experiment. The Gent model was discovered to be robust and mathematically simple when combined with physical basis. Moaleni et al(2018) developed stability and stress analysis of isotropic hyperelastic thick-walled pressure vessel which is an incompressible functionally graded material. The finite element method was applied to obtain the proposed analytical result. The FEM simulations and analytical solutions are reported to be in agreement. The results show that functionally graded material properties have a great effect on all stress components distribution throughout the thickness.

2.2 RELATED LITERATURE

Just like we are considering same hollow sphere and cylinder but with Levinson-Burgess strain energy function, the afore-mentioned also considered other strain energy function. The common ground remains that we all try to determine the different behaviour of these materials and we particularly dealt with the problem of determing the strain,stresses and displacements under internal pressure.

Erumaka(2003,2007,2007) considered finite deformation of incompressible solid of Ogden material deforming under anti-shear, finite deformation of an incompressible solid of Ogden material containing a line crack deforming under anti plane shear and finite deformation of a rotating sphere about its axis at a constant velocity respectively. The strain energy function of Ogden was considered for the three papers and closed form analytical solutions were sought and obtained for the determination of the displacements and stresses.

Sasso, Palmieri, Chiappini, and Amodio (2008) in their work on Characterization of hyperelastic rubber-like materials by biaxial and uniaxial stretching tests based on optical methods, conducted experimental rig to carry out equi-biaxial tests: the classic bulge test method has been coupled with optical devices allowing measurement in real time of the stress and elongation levels of the specimen. The material considered is said to be hyperelastic since it exhibits a particular stress-strain behaviour. FEM simulations of the test procedures gave a useful comparison between the numerical and experimental data.

Huang, Xie and Liu(2008) compared two types of strain energy density models for rubber material Mooney-Rivlin model and Yeoh model,and their material constants were analyzed using ANSYS

FEA software,the displacement and stress cloud atlases of the models were compared,and their applicability was verified, they concluded that Mooney-Rivlin model was suitable to simulate the behavior of medium and small strain,while Yeoh model was better suited for the behavior of large strain of NR filled with carbon black.

Goncalves, Pamploma, and Lopes(2008) investigated The shell used in the experiments composed of an isotropic, homogeneous and hyperelastic rubber, which is modeled as a Mooney-Rivlin incompressible material, described by two elastic constants. These constants are obtained by comparing the experimental and numerical solutions for the shell under axial tension. The large deformations of an extended thick cylindrical tube under internal pressure, with emphasis on the static nonlinear behavior and instabilities of the shell. Jianlong, Guangjuan, and Zhengwei(2008) introduced the two common strain energy density model of rubber material Mooney-Rivlin and Yeoh model,found the material constant,compared with the displacement and stress cloud of the two models by combining with Ansys finite element analysis software to verify their scope of application.

Hasanpour, Ziaei-Rad, and Mahzoon(2009) are more interested with formulation and constitutive equations of finite strain viscoelastic material using multiplicative decomposition in a thermodynamically consistent manner.the proposed constitutive equations were solved using finite element method(FEM). The main problem in generalizing constitutive models from small to finite deformations is to extend the theory in a thermodynamically consistent way, so that the second law of thermodynamics is preserved in every admissible process. This work is interested in the formulation and constitutive equations of finite strain viscoelastic material using multiplicative decomposition in a thermodynamically consistent manner. It is on this fact that the proposed

constitutive equations, a finite element (FE) procedure is developed and implemented in an FE code. Subsequently, the code is used to predict the response of elastomer bushings. The finite element analysis predicts displacements and rotations at the relaxed state reasonably well. The response to coupled radial and torsional deformations is also simulated.

Horgan and Murphy(2009, 2010) did similar work to that of Levinson and Burgess on Compression tests and constitutive models for the slight compressibilty of elastic rubber-like material. They investigated the role played by classical simple shear in nonlinear elasticity. They also determined the hydrostatic pressure for the particular case of neo-Hookean material and different stress distributions are compared and contrasted.

Maqueda(2010) developed new three-dimensional nonlinear dynamic rubber chains and belt drives models using the finite element absolute nodal coordinate formulation (ANCF) which enables for a straight forward implementation of general linear and nonlinear material models for structural elements such as beams, plates, and shells. This formulation, which is based on a more general kinematic description, can be used to predict the cross section deformation and its coupling with the extension and bending of the belt drives and rubber chains.

Altenbach and Eremeyev(2010) used direct approach to the plate theory where they focus was on an infinitesimal deformations of a plate consisting of hyperelastic materials. The high point was on their findings on the effect of initial stresses in the bulk material on the behaviour of the plate.

Andalaft-Chacur, Ali and Salazar (2011) introduced finite element method (FEM) and developed a numerical model for real options pricing problems. They established a Partial differential equation model, discretized the problem's domain by finite elements, obtained a weak formulation of the Partial differential equation and got the solution by solving the algebraic system.

There are a lot more FEM can do but we can concentrate on our main purpose of this work which is to practically implement the Levinson and Burgess strain energy function using Mathematica (ode45 solver).

There are Many Researchers who worked on the original natural rubber but it is obvious that there are many other rubber-like materials with same or similar mechanical properties.

Xiao, Yue and He(2011) used an explicit , exact method to ascertain multi-axial elastic potentials for isotropic rubber-like materials under large compressible deformations. They applied neo-Hookean hyperelastic materials as a case study in Hill's class. In 1978, Hill proposed a natural extension of Hooke's law to finite deformations. This paper showed a number of known Hookean type finite hyperelasticity models which are subjected to certain internal constraints. In order to solve the resulting equations, a novel idea of circumventing the strong nonlinearity was shown in a unified form for the whole class of elastic Hill materials.

Steinmann (2012) discovered that Rubber-like materials consist of chain-like macro-molecules that are more or less closely connected to each other via entanglements or cross-links. To achieve this research work, this particular structure was assumed as a completely random three-dimensional network. The elastic and nearly incompressible mechanical behaviour of this material class, numerous phenomenological and micro-mechanically motivated models were proposed in the literature. This contribution reviews fourteen selected representatives of these models, derives analytical stress–stretch relations for certain homogeneous deformation modes and summarises the details required for stress tensors and consistent tangent operators. The latter, although prevalently missing in the literature, are indispensable ingredients in utilising any kind of constitutive model for the numerical solution of boundary value problems by iterative approaches like the

Newton–Raphson scheme.

Koprowski-Theib, Johlitz, and Diebels(2012) in their paper deals with the investigations of a porous carbon black-filled rubber, tested with regard to its pressure and tension behaviour. In the tension range only uniaxial tests are performed while in the pressure range uniaxial as well as hydrostatic tests are performed. Wen and Zhao(2013) considered finite deformation for everted spherical shells composed of a class of isotropic incompressible Ogden materials. They derived a nonlinear equation explaining the relations among inner radius, initial thickness and material parameters of the spherical shell. They obtained the nonlinear equation describing the relations among inner radius, initial thickness and material parameters of the spherical shell. The numerical solutions obtained show that the inner radius of the everted spherical shell increases with the increasing initial thickness, the influences of the infinitesimal shear modulus μ_1 and the material constant α_1 on the inner radius are not significant.

Zehil and Garvin(2013) proposed a model that combines a selection of existing components that are known to reflect, with suitable accuracy, two main aspects of rubber behavior in finite strain rate-independent softening under deformation, also known as the Mullins effect, and hyper-viscoelasticity, including at high strain rates. The evolution model is further generalized to account for multiple rates of internal dissipation. Pascon and Coda(2013) worked on a shell finite element formulation to predict and solve the mechanical behaviour of highly deformable homogeneous elastic material.

Pucci and Saccomandi(2013) studied anti-plane shear motions for general and restricted Hadamard materials which are derived from the general Hadamard strain energy function. They assumed a constitutive parameterβ, to be equal to zero and they discovered the pure anti-plane shear motions

to be admissible solutions. A pure anti-plane motion may be sustained in Hadamard materials if β is not equal to zero only if combined with an in-plane motion. When β is very small, and by perturbing the system, approximate set of equations to actualize the in-plane motions which are associated with a Love wave in general Hadamard material are derived. The equations are determined by solving a set of linear diffrential equations from the time dependence.

Egbuhuzor and Eze(2013) considered the dynamic Reissner-Sagoci problem of incompressible solids where they used the strain energy function of Ogden material for the derivation of their second-order nonlinear differential equations. Closed form solution was achieved for displacements and stresses. Muamar, Bojan, Rabic, and Zoran(2014) said it also enables production of sheet metal components with complex contours by relatively low cost because only one rigid die is required. To produce a new component there are a trial and error stage to obtain a part without defects, which strongly depends on operator's experience. they opined that the experience of designer and manufacturers should give an important aid to reduce trials to realize the minimization of response time and cost with maximization of the product equality. Rubber pad forming highly improves the formability of the blank because the contact surfaces between the rigid die and the rubber pad is flexible. This method helped to produce sheet metal components with complex contour by relatively low cost because only one rigid die is required. the actualized this result by FE simulation of manufacturing process during the conceptual design.

Zhang, Li, and Xiao, (2014) applied the rational interpolation procedure and logarithmic strain, using a direct approach to obtain elastic potentials that exactly match uniaxial data and shear data for elastomers. This approach reduces the determination of multiaxial elastic potentials to that of two one-dimensional potentials, thus bypassing usual cumbersome procedures of identifying a

number of unknown parameters.

The work on obtaining multi-axial elastic potentials for rubber-like materials via an explicit, exact approach based on spline interpolation by Hao, Yuyu, Xiaoming, Zhengnam, and Heng(2014) proposed an explicit,exact approach to deduce multi-axial elastic potentials for isotropic rubber-like materials undergoing large incompressible deformations. This method reduces the problem of deriving multi-axial potentials to that of determining one-dimensional elastic potentials. This was actualized using a novel method based on certain logarithmic invariants. From the results, each of the multi-axial potentials exactly matched the finite strain data from four benchmark tests. Fosdick, Foti, Fraddosio, Marzano and Piccioni(2014) studied about toroidal twist-like biurcations for an isotropic Levinson-Burgess compressible elastic tube subjected to pure circular shear. They applied a novel effective method based on magnus expansion to analyze the bifurcation problem thereby evaluating the critical load.

Hao, Li and Liao(2015), improved on their previous work by applying method parameter identification and numerical simulations. The model was linearized geometrically and applied to incompressible rubbery materials and result show that their model can be used with large strains and not just for cases of loading. Aani and Rahimi(2015) obtained the stresses and displacements of axisymmetric radial deformation of the shell. Neo-Hookean strain energy function was applied to determine the behaviour of the material and results show that the outer and inner radius is a useful parameter which can be mirrored to certain applications to control the stresses. This is exactly why we are considering a case study of car tyre which is categorized as an artificial rubber and widely used for industrial purposes. De Pascalis, Abrahams, and Parnell (2015) presented a paper on Simple shear of a compressible quasilinear viscoelastic material published in the

International Journal of Engineering Science where they highlighted the effects of compressibility on the subsequent deformation and stress fields that result in this isochoric deformation, and calculations of the dissipated energy associated with both a ramp simple shear profile and oscillatory shear are given. To illustrate their results, they chose the compressible Neo-Hookean model proposed by Levinson and Burgess(1971) and from the result, the rates of deformation were found to be slow enough that inertia effects can be neglected. Giuseppe and Giuseppe(2015) reviewed important areas of Gent constitutive model for rubberlike materials. Their research was specifically based on damageable materials where they described certain damage and deformation localization. They observed that Gent behaves as the neo-Hookean model at low strain. The clear and simple mathematical structure of the Gent model allows one to possibly use generalized constitutive theories beyond classical Taylor expansions. Li and Wei(2015) examined four classic strain energy density (SED) functions for incompressible rubber-like materials, neo-Hookean, Mooney-Rivlin, Yeoh, and Ogden forms, are briefly reviewed. Yuan, Gu, Yin, and Xiao,(2015) established multi-axial hyper-elastic models for large strain rubberlike elasticity in a broad sense devoid of the commonly assumed constraint of incompressibility.Results are obtained directly from uniaxial stress-strain relations by means of certain explicit procedures and Novelties in four respects were achieved in the new models. Yukeler(2015) in their work on Theory of Rubber-like Rods presented a theory for incompressible rubber-like straight rods undergoing finite strains and finite rotations. Strains are expanded asymptotically for transverse coordinate of undeformed rod. The equations of equilibrium and corresponding boundary conditions are obtained by implementing minimum total potential energy principle. Necessary conditions for the satisfaction of the stress-free boundary conditions on the top and bottom free surfaces of the rubber-like rods

are derived. For the illustration and test of the proposed theory, the flexural buckling problem of Mooney–Rivlin rods under axial compressive loads is considered.The paper is restricted with the straight rods where ϕ is constant. It can be extended to the curved rods by considering ϕ as a function of s in a later study. Hao, et al (2015) ,showed an important dependence of predeformation of filled rubber-like materials. They investigated the role of frequency and applitude when loaded with static predeformations superimposed by harmonic deformations. The constitutive equations were geometrically linearized in the neighbourhood of predeformation and formulated for incompressible materials.They showed some numerical results as they process the parameter identification. The results show that their model also be applied to large strains and not just on small strains.

Shahzad, Kamran, Siddiqui, and Farhan(2015). characterized hyperelastic material and also obtained a better strain energy function for an indigenously developed rubber which will be applied in flexible joint use for thrust vectoring of solid rocket motor. Digital image correlation (DIC) technique was applied to have strain measurements for biaxial and planar specimens to input stress-strain data in Abaqus®. Yeoh model seems to be right choice, among the available material models, because of its ability to match experimental stress-strain data at small and large strain values. Quadlap specimen test was administered to validate material model fitted from test data. FE simulations were carried out to verify the behavior as predicted by Yeoh model and results are found to be in good agreement with the experimental data.

Ivanov and Nikolova(2016) used nonlinear second-order ordinary differential equation to examine the inflation of a thin-walled hyperelastic spherical membrane undergoing internal pressure. They determined the stability of equilibria of the basic model applying three different types of strain

energy functions(SEFs) and proved analytically that a stable inflation of the membrane can retain or change to an unstable one depending on the particular analytical form of SEF and its material parameters.

Mangan, Destrade, and Saccommandi(2016) obtained the strain energy function for isotropic incompressible solids solids exhibiting a linear relationship between shear stress and amount of shear and between torque and amount of twist when under large simple shear or torsion deformation.This model is chosen in an effort to obtain the strain-hardening effects which happen for moderate to large extensions of rubber, and which cannot be deduced by the Mooney-Rivlin model alone.

Zhao(2016) derived a partial differential equation for isotropic hyperelastic constitutive models from stored energy and stress work done. He used the Lie group approach to solve the partial differential equation which are functions of three invariants. The particular solution was applied for several isotropic hyperelastic materials.

One of the most effective numerical tool is finite element method,even though we are not using it as a numerical tool for solution of our problem. Finite element method can be used for hyper-elastic material such as rubber to estimate the temperature rise during cyclic loading. The work by Puglisi and Saccomandi(2016) on modeling of rubber-like materials and soft tissues shows that it is possible to practical obtain mathematical models for the behaviour of these materials using mesoscopic information.

Puglisi (2016) discussed the multi-scale methods for modelling of rubber-like and soft tissues and then compare them with classical macroscopic phenomenological models. He opined that the behaviour of such materials is quite difficult to predict because rubber self-organizes into

mesoscopic physical structures that play a prominent role in determining their complex, history-dependent and strongly nonlinear response. multi-scale approaches were found to be important for theoretical comprehension and prediction of the complex mechanical response of these materials.

Sang, Xing, Liu, Li, Wang, and Lv(2016) worked on rubber tubes under pressure undergoing large deformation and present a specific nonlinear elastic behaviour. They established a connection between internal pressure and the internal volume ratio.

Wriggers(2016) Finite element methods for solving engineering problems. They presented the basic continuum formulation and different discretization techniques that can be used to overcome the engineering problems. Mathematical computation is one of the trending tools to solving some numerical challenges not just in Engineering, biological sciences but also in finance. Lev and Volokh(2016) focused on a new form of the strain energy function which describes the elastic behaviour of rubber-like materials undergoing numerous deformation. Their respective results show good agreement between model and experimental data obtained for all materials. Ahmed and Mark(2017) wrote on new weight function based(WFB) which they explained the stress-strain behaviour of the hyperelastic materials. This newly proposed approach has been proved against the Treolar's vulcanized rubber material and compared to Ogden and Yeoh's methods and it is said to be more accurate for uniaxial tension since it has an error value less than that of Ogden and Yeoh models by 1.0 to 39percent. Levyakov(2017) considered the problem of nonlinear bending of a curved tube comprising of incompressible rubber-like material. A change in the tube due to bending is observed in the derivation of governing equations. The effect of pressure on the bending stiffness, stability, and deformations of a curved tube is checked and discussed. Adel, Makrem,

Abdelmalek, Adel, Jale, and Mohammed (2017) developed a three dimensional viscoelastic model at finite strain to describe nonfactorizable behavior of rubber-like materials.The proposed model is able to reproduce quasi-static response and exhibit ability to predict the dynamic response of nonfactorizable rubber-like materials (BIIR) and the multi-integral model of Pipkin in a wide range of strain. Aani and Rahimi(2018) in their paper, worked on the stability of thick-walled spherical and cylindrical shells made of functionally graded(FG) incompressible hyperelastic material undergoing internal pressure, the strain energy function function of extended Ogden material with variable material parameter was applied to model the behaviour of the material.

Result shows that the material inhomogeneity parameter and shell thickness have an important influence on the stability of the material. FE simulations were used to study behaviour as predicted by Yeoh model and result were discovered to be in good agreement with the experimental data.

Yaya and Bechir(2018) presented a new hyper-elastic model that is based on the standard invariants of Green-Cauchy. Experimental data reported by Treloar are used to identify the model parameters. The new model has four material parameters , their identification leads to linear optimization problem and it is able to predict multi-axial behaviour of rubber-like materials. They investigated the inflation of a rubber balloon with the new model and Ogden models and compared both the analytic and numerical solutions derived from these models.

Valiollahi, Shojaeifard, and Baghan(2019) in this work on closed form solutions for large deformation of cylider under combined extension-torsion obtained a closed form analytical solution for extension-torsion of a hyperelastic cylinder . Analytical method for stretch based strain energy function was considered and finite element method was used on ABAQUS to verify the analytical methods used. The finite element results for stress distribution show a good

agreement with analytical findings which validates the accuracy of the proposed method. For stretches smaller than theis alteration point, the cylinder always elongates while for larger stretches, the cylinder shortens for small twists and then elongates on further twisting.

Kulcu(2019) in his contribution proposed a new strain energy function to describe the hyperelastic behaviour of rubber-like materials under various deformation. The proposed strain energy function represents an invariant based model which has two material constants. This model was tested with the experimental data of vulcanized rubbers, collagen and fibrin. The parameters were kept constant when placed under certain types of loads. There was an agreement between the model and the experimental data for all materials.

Egbuhuzor and Erumaka(2020) investigated the finite deformation of internally pressurized spherical compressible rubber-like material. The Levison-Burgess strain energy function was considered and they derived a second-order nonlinear ordinary differential equation with its boundary conditions. The problem was solved numerically using collocation and shooting methods to calculate the displacements and stresses at different points. Statistical analysis was also applied to analyze the error difference between the two methods.

2.3 SPECIFIC LITERATURE

We review the following known results which we shall need later for the conclusion and validation of our results in chapter four.

- Blatz and Ko(1962):

  Blatz and Ko(1962) in their work proposed a strain energy function which they called ”Standard” strain energy function but Levinson and Burgess(1971) discovered that there

were certain limitations. First, in the limit of incompressibility, the standard strain energy function cannot represent Mooney-Rivlin or Neo-Hookean material and secondly, It is not a capable strain energy function for an isotropic material. Based on these facts, Levinson and Burgess introduced the simplest rational polynomial strain energy function as shown in equation(1).

- Chung, Horgan, and Abeyaratne(1986):

  Chung et al(1986) in their work on the finite deformation of internally pressurized hollow cylinders and spheres for a class of compressible elastic materials considered hollow circular cylinders and spheres deorming under applied internal pressure condition for the initiation of localized shear bifurcation. It is shown that when the ratio of the outer undeformed radius to the inner undeformed radius is larger than the critical value, the shear bifurcation occurs before the maximum pressure is reached, while when the ratio is smaller than the critical value, the converse is true. This analysis was carried out for a particular compressible elastic foam rubber material(Blatz-Ko). This strain energy function was derived from the work of Blatz and Ko(1962). They derived a boundary value model equatrion using condition for foam rubber. The resulting second order ordinary differential equations are solved in closed form for the determination of the displacement distributions.

- Horgan(1996):

  Horgan(1996) in his research worked on remarks on ellipticity for the generalized Blatz-Ko constitutive model for a compressible nonlinearly elastic solid. They presented an expression for strain energy density per unit undeformed volume for homogeneous isotropic elastic

compressible material given by:

$$W = \frac{\mu}{2} f\Big[I_1 - 1 - \frac{1}{v} + \frac{(1-2v)}{v} I_3{}^{\frac{-v}{(1-2v)}}\Big] + \frac{\mu}{2}(1-f)\Big[\frac{I_2}{I_3} - 1 - \frac{1}{v} + \frac{(1-2v)}{v} I_3{}^{\frac{v}{1-2v}}\Big] \quad (2.1)$$

where μ, v and f are such that $\mu > 0$,$0 \leq f \leq 1$, $0 < v < \frac{1}{2}$.

The constraints μ, v are the shear modulus and Poisson's ratio for infinitesimal deformations while f is related to the volume fraction of voids in the foam-rubber material model. The above model is known as generalized Blatz-Ko material and was first proposed by Blatz and Ko(1962).

Horgan placed two special conditions on equation 2.1 namely when $f = 0$ and $f = 1$ respectively.

Condition A($f = 0$):

$$W = \frac{\mu}{2}\Big[\frac{I_2}{I_3} - 1 - \frac{1}{v} + \frac{(1-2v)}{v} I_3{}^{\frac{v}{1-2v}}\Big] \quad (2.2)$$

Condition B ($f = 1$):

$$W = \frac{\mu}{2} f\Big[I_1 - 1 - \frac{1}{v} + \frac{(1-2v)}{v} I_3{}^{\frac{-v}{(1-2v)}}\Big] \quad (2.3)$$

Considering $v = \frac{1}{4}$ for both equations 2.2 and 2.3 they obtained;

$$W = \frac{\mu}{2}(\frac{I_2}{I_3} - 2I_3{}^{\frac{1}{2}} - 5) \quad (2.4)$$

Also, limit as I_3 tends to 1, 2.1 yields

$$W = \frac{\mu}{2} f(I_1 - 3) + \frac{\mu}{2}(1 - f)(I_2 - 3) \tag{2.5}$$

2.5 is the well known Mooney Rivlin strain energy density for incompressible materials while 2.2 is the compressible generalization of neo-Hookean incompressible material $2W = \mu(I_1 - 3)$.

Also, if $I_1 = 3$, $I_2 = 3$ and $I_3 = 1$, 2.1 varnishes in the undeformed reference state. The work by Bolzon and Vitaliani(1993) drew attention to 2.4 and **??** without realizing realizing that their model is similar to that of the generalized Blatz-Ko material as captured by Horgan(1996) in 2.1.

- Levinson and Burgess(1971):

  We are more concerned with the synthetic rubber which is a solid rubber and also referred to as artificial rubber.The main interest and motivation came from the work done by Levinson and Burgess (1971). They proposed a strain energy function which they called polynomial compressible materials and went further to examine the behaviour of Blatz, Blatz-Ko and their proposed material under various loading conditions just to obtain their respective behaviour of the patterns.

  Hence, the experimental value shows that for a synthetic rubber-like material, $f = 1$ and $v = 0.46$, we obtained the strain energy function for a compressible material. At this point, equation(1.1) reduces to;

$$W = \frac{\mu_0}{2}\left[I_1 - 27\sqrt{I_3} + \frac{25}{2}I_3 + \frac{23}{2}\right] \tag{2.6}$$

Levinson and Burgess(1971) were primarily concerned with the strain energy function of a highly compressible polyurethane foam rubber for which they found experimentally that $f = 0$ and $v = 0.25$ but for a solid rubber of the same chemical composition, it was found that$f = 1$and $v = 0.46$. Since for the incompressible case the I and J invariants become identical, compressible generalizations of the neo-Hookean and Mooney-Rivlin material clearly may be made in terms of either set of invariants.

The strain energy density for a compressible hyperelastic material in equation (1.1) which reduces to the Mooney-Rivlin material as v tends to 0.5 was also obtained in Horgan(1996)

The difference between these literatures and our work is the fact that none to our knowledge has investigated the usefulness of the strain energy function of Levinson and Burgess in determining the displacements and stresses of deformations involving both the spherical and cylindrical coordinate systems. Levinson and Burgess compared other strain energy functions using the poisson ratio and material constant to determine the behaviour of the materials. Levinson and Burgess(1971), in their work considered five stress fields:

(i) uniaxial tension;

(ii) equal biaxial plane stress;

(iii) hydrostatic stress ;

(iv) equal biaxial plane strain; and

(v) uniaxial strain

All of the loadings considered have a high degree of symmetry. The equations describing these relations are all derived from the finite elastic constitutive relation.

- Remark:

  This work is another dimension to the work done by Levinson and Burgess(1971). We considered the problem as a hollow sphere and hollow cylinder similar to the work of Blatz and Ko(1962,1986). The difference beetween our work and Blatz and Ko(1962,1986) is that they considered the strain energy function of foam rubber($f = 0$ and $v = 0.25$). Similarly, Levinson and Burgess(1971) in their work also focused only on highly compressible foam rubber. In this work, we considered the strain energy function when $f = 1$ and $v = 0.46$ which is said to be a solid(synthetic) rubber and we derived the equation of the strain energy function as shown in (2.6). We also derived the second order nonlinear ordinary differential equations with appropriate boundary value conditions which were simulated using mathematica software for the determination of stresses and displacements.

Chapter 3

METHODLOGY

3.1 SPHERICAL POLAR COORDINATES:

Considering the deformation of a spherical hollow sphere that takes the point with the spherical polar coordinates (R, Θ, Φ) in the undeformed region to the point (r, θ, ϕ) in the deformed region such that;

$$r = r(R) \qquad a \leq R \leq b$$

$$\theta = \Theta \qquad 0 \leq \Theta \leq \pi$$

$$\phi = \Phi \qquad 0 \leq \Phi \leq 2\pi$$

$$\frac{dr}{dR} > 0$$

$r(R)$ is a continuously differentiable function to be determined and deformation gradient tensor,$\overline{\mathrm{F}}$ is given by

Figure 3.1: Hollow Sphere

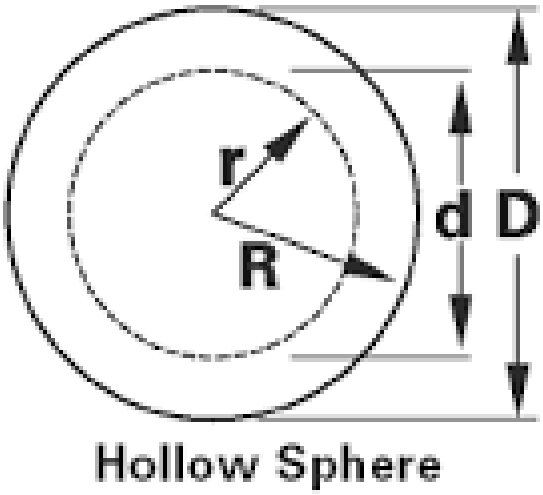

$$\overline{\mathrm{F}} = \begin{bmatrix} (\frac{dr}{dR}) & 0 & 0 \\ 0 & (\frac{r}{R}) & 0 \\ 0 & 0 & (\frac{r}{R}) \end{bmatrix} \tag{3.1}$$

$F = diag(\frac{dr}{dR}, \frac{r}{R}, \frac{r}{R})$

3.1.1 DEVELOPMENT OF FIELD EQUATION

PRINCIPAL STRETCHES

Principal stretches are the eigenvalues of F which from equation(3.1) are given as: $\lambda_1 = \frac{dr}{dR}$, $\lambda_2 =$

$\lambda_3 = \frac{r}{R}$.

Cauchy Green Right Tensor

$$\overline{\mathrm{F}}^T = \begin{bmatrix} (\frac{dr}{dR}) & 0 & 0 \\ 0 & (\frac{r}{R}) & 0 \\ 0 & 0 & (\frac{r}{R}) \end{bmatrix} \tag{3.2}$$

Multiplying equations (3.1) and (3.), we obtain the right Cauchy Green tensor $\overline{\mathrm{C}}$

$$\overline{\mathrm{F}}^T\overline{\mathrm{F}} = \begin{bmatrix} \frac{dr}{dR} & 0 & 0 \\ 0 & \frac{r}{R} & 0 \\ 0 & 0 & \frac{r}{R} \end{bmatrix} \begin{bmatrix} \frac{dr}{dR} & 0 & 0 \\ 0 & \frac{r}{R} & 0 \\ 0 & 0 & \frac{r}{R} \end{bmatrix}$$

$$\overline{\mathrm{C}} = \overline{\mathrm{F}}^T\overline{\mathrm{F}} = \begin{bmatrix} (\frac{dr}{dR})^2 & 0 & 0 \\ 0 & (\frac{r}{R})^2 & 0 \\ 0 & 0 & (\frac{r}{R})^2 \end{bmatrix} \tag{3.3}$$

The Principal Invariants:

I_1, I_2, I_3, are given as:

$$I_1 = tr\overline{\mathrm{C}} = (\frac{dr}{dR})^2 + 2(\frac{r}{R})^2, \tag{3.4}$$

$$(tr\overline{\mathrm{C}})^2 = \big[(\tfrac{dr}{dR})^2 + 2(\tfrac{r}{R})^2\big]^2$$

$$tr\overline{\mathrm{C}}^2 = ((\tfrac{dr}{dR}^2)^2 + 4((\tfrac{r}{R})^2))^2$$

$$I_2 = \frac{1}{2}\Big[(tr\overline{\mathrm{C}})^2 - (tr\overline{\mathrm{C}}^2)\Big] = 2(\frac{dr}{dR})^2[\frac{r^2}{R^2} + \frac{r^4}{R^4}] \tag{3.5}$$

$$I_3 = det\overline{\mathrm{C}} = (\frac{dr}{dR})^2(\frac{r}{R})^4 \tag{3.6}$$

Cauchy Stresses (σ_{ij}) :

According to the principle of conservation of angular momentum, equilibrium requires that the summation of moments with respect to an arbitrary point is zero, which leads to the conclusion that the stress tensor is symmetric. The Cauchy stress is called the true stress, to distinguish it from other stress tensors. It is called the true stress because it is a true measure of the force per unit area in the deformed configuration and the Cauchy stress is the sensible way of describing the action of surface forces. From Cauchy elasticity, according to Horgan(1986), we have;

$$\sigma_{ii} = \frac{\lambda_i}{\lambda_1\lambda_2\lambda_3}\frac{\partial W}{\partial \lambda_i}, \tag{3.7}$$

for i = 1,2,3.

where W is the strain energy function of the material to be considered. Recall that :

$$W = \frac{\mu_0}{2}\left[I_1 - 27\sqrt{I_3} + \frac{25}{2}I_3 + \frac{23}{2}\right] \tag{3.8}$$

$$I_1 = \lambda_1^2 + \lambda_2^2 + \lambda_3^2 \tag{3.9}$$

$$I_3 = {\lambda_1}^2{\lambda_2}^2{\lambda_3}^2 \tag{3.10}$$

$$\frac{\partial W}{\partial \lambda_1} = \frac{\mu_0}{2}\frac{\partial\left[{\lambda_1}^2 + {\lambda_2}^2 + {\lambda_3}^2 - 27\sqrt{{\lambda_1}^2{\lambda_2}^2{\lambda_3}^2} + \frac{25}{2}{\lambda_1}^2{\lambda_2}^2{\lambda_3}^2 + \frac{23}{2}\right]}{\partial \lambda_1} \tag{3.11}$$

$$\frac{\partial W}{\partial \lambda_2} = \frac{\mu_0}{2} \frac{\partial \left[{\lambda_1}^2 + {\lambda_2}^2 + {\lambda_3}^2 - 27\sqrt{{\lambda_1}^2 {\lambda_2}^2 {\lambda_3}^2} + \frac{25}{2} {\lambda_1}^2 {\lambda_2}^2 {\lambda_3}^2 + \frac{23}{2} \right]}{\partial \lambda_2} \tag{3.12}$$

$$\frac{\partial W}{\partial \lambda_3} = \frac{\mu_0}{2} \frac{\partial \left[{\lambda_1}^2 + {\lambda_2}^2 + {\lambda_3}^2 - 27\sqrt{{\lambda_1}^2 {\lambda_2}^2 {\lambda_3}^2} + \frac{25}{2} {\lambda_1}^2 {\lambda_2}^2 {\lambda_3}^2 + \frac{23}{2} \right]}{\partial \lambda_3} \tag{3.13}$$

$$\sigma_{11} = \sigma_{rr} = \frac{1}{\lambda_2 \lambda_3} \frac{\mu_0}{2} \frac{\partial}{\partial \lambda_1} \left[{\lambda_1}^2 + {\lambda_2}^2 + {\lambda_3}^2 - 27\sqrt{{\lambda_1}^2 {\lambda_2}^2 {\lambda_3}^2} + \frac{25}{2} {\lambda_1}^2 {\lambda_2}^2 {\lambda_3}^2 + \frac{23}{2\lambda_2 \lambda_3} \right] \tag{3.14}$$

$$\sigma_{11} = \frac{\mu_0}{2} \frac{\partial}{\partial \lambda_1} \left[\frac{{\lambda_1}^2}{\lambda_2 \lambda_3} + \frac{\lambda_2}{\lambda_3} + \frac{\lambda_3}{\lambda_2} - 27\lambda_1 + \frac{25{\lambda_1}^2 \lambda_2 \lambda_3}{2} + \frac{23}{2\lambda_2 \lambda_3} \right] \tag{3.15}$$

$$\sigma_{11} = \frac{\mu_0}{2} \left[\frac{2\lambda_1}{\lambda_2 \lambda_3} + 25\lambda_1 \lambda_2 \lambda_3 - 27 \right] \tag{3.16}$$

$$\sigma_{11} = \frac{\mu_0}{2} \left[\frac{2r'}{r^2} R^2 + \frac{25r'}{R^2} r^2 - 27 \right] \tag{3.17}$$

$$\frac{\partial W}{\partial \lambda_2} = \frac{\mu_0}{2} \frac{\partial \left[{\lambda_1}^2 + {\lambda_2}^2 + {\lambda_3}^2 - 27\sqrt{{\lambda_1}^2 {\lambda_2}^2 {\lambda_3}^2} + \frac{25}{2} {\lambda_1}^2 {\lambda_2}^2 {\lambda_3}^2 + \frac{23}{2} \right]}{\partial \lambda_2} \tag{3.18}$$

$$\sigma_{22} = \sigma_{33} = \sigma_{\phi\phi} = \sigma_{\theta\theta} = \frac{1}{\lambda_1\lambda_3}\frac{\mu_0}{2}\frac{\partial}{\partial\lambda_1}\left[{\lambda_2}^2 + {\lambda_2}^2 + {\lambda_3}^2 - 27\sqrt{{\lambda_1}^2{\lambda_2}^2{\lambda_3}^2} + \frac{25}{2}{\lambda_1}^2{\lambda_2}^2{\lambda_3}^2 + \frac{23}{2\lambda_2\lambda_3}\right] \tag{3.19}$$

$$\sigma_{22} = \sigma_{33} = \sigma_{\theta\theta} = \sigma_{\phi\phi} = \frac{\mu_0}{2}\left[\frac{2}{r'} + \frac{25r'}{R^2}r^2 - 27\right] \tag{3.20}$$

$$\sigma_{r\theta} = \sigma_{\theta r} = \sigma_{\theta\phi} = \sigma_{\phi\theta} = \sigma_{r\phi} = \sigma_{\phi r} = 0 \tag{3.21}$$

3.1.2 EQUILIBRIUM EQUATIONS IN SPHERICAL COORDINATES SYSTEM

The equation of static deformation of spherical shaped bodies have been developed by Mohammed & Rahman in 2014 as:

$$\frac{\partial\sigma_{rr}}{\partial r} + \frac{1}{r}\frac{\partial\sigma_{\theta r}}{\partial\theta} + \frac{1}{r\sin\theta}\frac{\partial\sigma_{\phi r}}{\partial\phi} + \frac{1}{r}(2\sigma_{rr} - \sigma_{\theta\theta} - \sigma_{\phi\phi} + \sigma_{\theta r}\cot\theta) + f_r = 0 \tag{3.22}$$

$$\frac{\partial\sigma_{r\theta}}{\partial r} + \frac{1}{r}\frac{\partial\sigma_{\theta\theta}}{\partial\theta} + \frac{1}{r\sin\theta}\frac{\partial\sigma_{\theta\phi}}{\partial\phi} + \frac{1}{r}(3\sigma_{r\theta} + (\sigma_{\theta\theta} - \sigma_{\phi\phi})\cot\theta) + f_\theta = 0 \tag{3.23}$$

$$\frac{\partial \sigma_{r\phi}}{\partial r} + \frac{1}{r}\frac{\partial \sigma_{\theta\phi}}{\partial \theta} + \frac{1}{r\sin\theta}\frac{\partial \sigma_{\phi\phi}}{\partial \phi} + \frac{1}{r}(3\sigma_{r\phi} + (\sigma_{\theta\theta} - \sigma_{\theta\phi}\cot\theta) + f_{\phi} = 0 \tag{3.24}$$

Recall the Cauchy first law of continuum mechanics where there is equilibrium and no body force;

$$div\sigma_{ij} = 0 \tag{3.25}$$

where f_r, f_θ and f_ϕ represent the body forces which are all zero. We are to consider the spherical coordinates taking into cognizance the fact that we are dealing with symmetric deformations. Applying the Cauchy stresses and transforming the obtained equilibrium equation, we have;

$$\frac{d\sigma_{rr}}{dR} + \frac{2r'}{r}\Big[\sigma_{rr} - \sigma_{\theta\theta}\Big] = 0, \tag{3.26}$$

$$r' = \tfrac{dr}{dR}$$

Applying the stresses from equations 3.17, 3.20 and 3.21 into equation 3.26 and solving the derivative we obtain the model equation for the spherical deformation of a synthetic rubber;

$$\sigma_{11} = \Big[\frac{2r'}{r^2}R^2 + \frac{25r'}{R^2}r^2 - 27\Big] \tag{3.17}$$

$$\sigma_{22} = \sigma_{33} = \sigma_{\theta\theta} = \sigma_{\phi\phi} = \frac{\mu_0}{2}\Big[\frac{2}{r'} + \frac{25r'}{R^2}r^2 - 27\Big] \tag{3.20}$$

$$\sigma_{r\theta} = \sigma_{\theta r} = \sigma_{\theta\phi} = \sigma_{\phi\theta} = \sigma_{r\phi} = \sigma_{\phi r} = 0 \tag{3.21}$$

$$\sigma_{rr} = \Big[\frac{2r'}{r^2}R^2 + \frac{25r'}{R^2}r^2 - 27\Big] \tag{3.7}$$

$$\frac{d(\mu(\frac{r'R^2}{r^2} + \frac{25r'r^2}{R^2} - 27)}{dR} + \mu\frac{2r'}{r}\Big[\frac{r'R^2}{r^2} + \frac{25r'r^2}{R^2} - 27 - (\frac{2}{r'} + \frac{25r'r^2}{R^2} - 27)\Big] = 0, \tag{3.27}$$

$$\mu\Big[\frac{d(\frac{2r'R^2}{r^2} + \frac{2r'r^2}{R^2} - 27)}{dR} + (\frac{4r'^2R}{r^3} - \frac{4}{r})\Big] = 0, \tag{3.28}$$

$$\frac{\mu}{2}\Big[\frac{2r''R - 2rr' - 4(r')^2R}{r^3} + \frac{25r''r^2R + 50r'^2rR - 50r'r^2}{R^3} + (\frac{4r'^2R}{r^3} - \frac{4}{r})\Big] = 0 \tag{3.29}$$

$$\frac{2rr''R^4 + 2rr'R^3 - 4r'^2R^4 + 25r''r^5R + 50r'^2r^4R - 50r'r^5 + 4r'^2R^4 - 4r^2R^3}{r^3R^3} = 0 \tag{3.30}$$

Note that $\mu \neq 0$, Also, $r^3R^3 \neq 0$ Therefore,the above equation becomes;

$$r''(2rR^4 + 25r^5R) + 50r'^2r^4R + r'(2rR^3 - 50r^5) - 4r^2R^3 = 0, \tag{3.31}$$

Equation (3.1.25) can further be represented as:

$$(2R^4 + 25r^4R)\frac{d^2r}{dR^2} + 50r^3R(\frac{dr}{dR})^2 + (4R^3 - 50r^4)\frac{dr}{dR} - 2rR^3 = 0 \tag{3.32}$$

3.1.3 BOUNDARY VALUE MODEL EQUATION OF SPHERICALLY SYMMETRIC DEFORMATION

Now consider a spherical hollow rubber-like material of Levinso-Burgess strain energy function deforming under internal pressure of magnitude such that the external surface is stress free.

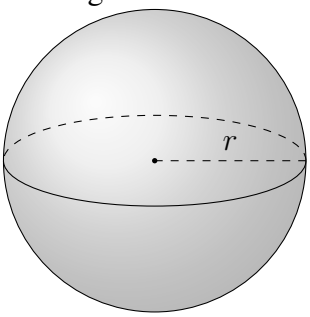

For this case the boundary conditions are;

$(\sigma_{rr})_{R=a} = -\rho$ and $(\sigma_{rr})_{R=b} = 0$

Applying the conditions of a hollow sphere on the radial stress, we obtain the following boundary conditions as;

$$(\sigma_{rr})_{R=a} = -\rho \implies \frac{\mu_0}{2}\Big[\frac{2r'a^2r^2}{+}\frac{25r'r^2}{a^2} - 27\Big] = -\rho r'(a) = \frac{a^2r^2(a)(27\mu_0 - 2\rho)}{\mu_0(2a^4 + 25r^4(a))} \tag{3.33}$$

Applying the second condition,

$$(\sigma_{rr})_{R=b} = -\rho \implies \frac{\mu_0}{2}\Big[\frac{2r'}{r^2}b^2 + \frac{25r'}{b^2}r^2 - 27\Big] = 0 \tag{3.34}$$

$$(\sigma_{rr})_{R=b} = 0 \implies r'(b) = \frac{27b^2r^2(b)}{2b^4 + 25r^4(b)} \tag{3.35}$$

Hence, we are set to solve the boundary value problem;

$$(2R^4 + 25r^4R)\frac{d^2r}{dR^2} + 50r^3R(\frac{dr}{dR})^2 + (4R^3 - 50r^4)\frac{dr}{dR} - 2rR^3 = 0 \tag{3.32}$$

$$r'(a) = \frac{a^2r^2(a)(27\mu_0 - 2\rho)}{\mu_0(2a^4 + 25r^4(a))} \tag{3.33}$$

$$r'(b) = \frac{27b^2r^2(b)}{2b^4 + 25r^4(b)} \tag{3.35}$$

3.2 FIELD EQUATION FOR SYMMETRIC DEFORMATION OF A CYLINDRICAL MATERIAL OF LEVINSON-BURGESS

We consider the case of deformation that takes the point (R, Θ, Z) of the cylinder in the undeformed configuration to (r, θ, z) in the deformed configuration such that

this represents a three dimensional cross-section of a solid cylinder with an internal and external radii a and b in its undeformed form.

$$r = r(R) \qquad a \leq R \leq b$$

$$\theta = \Theta \qquad 0 \leq \Theta \leq 2\pi$$

$$z = Z\gamma \qquad 0 \leq Z \leq l$$

$$\frac{dr}{dR} > 0$$

where γ is a material constant

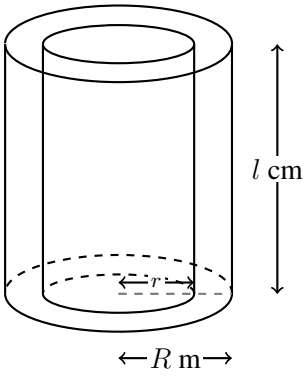

For this case, the deformation gradient tensor $\overline{\mathrm{F}}$ is given by;

$$\overline{\mathrm{F}} = \begin{bmatrix} (\frac{dr}{dR}) & 0 & 0 \\ 0 & (\frac{r}{R}) & 0 \\ 0 & 0 & (\gamma) \end{bmatrix} \tag{3.1}$$

where $\overline{\mathrm{F}} = \overline{\mathrm{F}}^T$

$$\overline{\mathrm{F}}^T\overline{\mathrm{F}} = \begin{bmatrix} \frac{dr}{dR} & 0 & 0 \\ 0 & \frac{r}{R} & 0 \\ 0 & 0 & \gamma \end{bmatrix} \begin{bmatrix} \frac{dr}{dR} & 0 & 0 \\ 0 & \frac{r}{R} & 0 \\ 0 & 0 & \gamma \end{bmatrix}$$

3.2.1 CAUCHY GREEN RIGHT TENSOR

$$\overline{\mathrm{C}} = \overline{\mathrm{F}}^T\overline{\mathrm{F}} = \begin{bmatrix} (\frac{dr}{dR})^2 & 0 & 0 \\ 0 & (\frac{r}{R})^2 & 0 \\ 0 & 0 & (\gamma)^2 \end{bmatrix} \tag{3.2}$$

3.2.2 THE PRINCIPAL INVARIANTS

$$I_1 = tr\overline{\mathrm{C}} = (\frac{dr}{dR})^2 + (\frac{r}{R}) + (\gamma)^2, \tag{3.3}$$

$$I_2 = \frac{1}{2}\Big[(tr\overline{\mathrm{C}})^2 - tr(\overline{\mathrm{C}})^2\Big] = (\frac{r}{R})^2(\frac{dr}{dR})^2 + (\frac{r^2\gamma^2}{R^2}) + (\gamma)^2(\frac{dr}{dR})^2, \tag{3.4}$$

$$I_3 = det\overline{\mathrm{C}} = (\frac{dr}{dR})^2(\frac{r}{R})^2(\gamma)^2 \tag{3.5}$$

3.2.3 CAUCHY STRESSES

Using Cauchy tensor as defined in equation (3.7);

$$\sigma_{ii} = \frac{\lambda_i}{\lambda_1\lambda_2\lambda_3}\frac{\partial W}{\partial \lambda_i}, \qquad \text{for i = 1,2,3}$$

$$\frac{\partial W}{\partial \lambda_1} = \frac{\mu_0}{2}\frac{\partial\left[{\lambda_1}^2 + {\lambda_2}^2 + {\lambda_3}^2 - 27\sqrt{{\lambda_1}^2{\lambda_2}^2{\lambda_3}^2} + \frac{25}{2}{\lambda_1}^2{\lambda_2}^2{\lambda_3}^2 + \frac{23}{2}\right]}{\partial\lambda_1} \tag{3.6}$$

$$\frac{\partial W}{\partial \lambda_2} = \frac{\mu_0}{2}\frac{\partial\left[{\lambda_1}^2 + {\lambda_2}^2 + {\lambda_3}^2 - 27\sqrt{{\lambda_1}^2{\lambda_2}^2{\lambda_3}^2} + \frac{25}{2}{\lambda_1}^2{\lambda_2}^2{\lambda_3}^2 + \frac{23}{2}\right]}{\partial\lambda_2} \tag{3.7}$$

$$\frac{\partial W}{\partial \lambda_3} = \frac{\mu_0}{2}\frac{\partial\left[{\lambda_1}^2 + {\lambda_2}^2 + {\lambda_3}^2 - 27\sqrt{{\lambda_1}^2{\lambda_2}^2{\lambda_3}^2} + \frac{25}{2}{\lambda_1}^2{\lambda_2}^2{\lambda_3}^2 + \frac{23}{2}\right]}{\partial\lambda_3} \tag{3.8}$$

$$\sigma_{11} = \sigma_{rr} = \frac{\lambda_1}{\lambda_1\lambda_2\lambda_3}\frac{\mu_0}{2}\frac{\partial}{\partial\lambda_1}\left[{\lambda_1}^2 + {\lambda_2}^2 + {\lambda_3}^2 - 27\sqrt{{\lambda_1}^2{\lambda_2}^2{\lambda_3}^2} + \frac{25}{2}I_3 + \frac{23}{2}\right] \tag{3.9}$$

$$\sigma_{11} = \sigma_{rr} = \frac{1}{\lambda_2\lambda_3}\frac{\mu_0}{2}\frac{\partial}{\partial\lambda_1}\left[{\lambda_1}^2 + {\lambda_2}^2 + {\lambda_3}^2 - 27\sqrt{{\lambda_1}^2{\lambda_2}^2{\lambda_3}^2} + \frac{25}{2}{\lambda_1}^2{\lambda_2}^2{\lambda_3}^2 + \frac{23}{2\lambda_2\lambda_3}\right] \tag{3.10}$$

$$\sigma_{11} = \frac{\mu_0}{2}\frac{\partial}{\partial\lambda_1}\Big[\frac{{\lambda_1}^2}{\lambda_2\lambda_3} + \frac{\lambda_2}{\lambda_3} + \frac{\lambda_3}{\lambda_2} - 27\lambda_1 + \frac{25{\lambda_1}^2\lambda_2\lambda_3}{2} + \frac{23}{2\lambda_2\lambda_3}\Big] \tag{3.11}$$

$$\sigma_{11} = \sigma_{rr} = \frac{\mu_0}{2}\Big[\frac{2r'}{r\gamma}R + \frac{25r'\gamma}{R}r - 27\Big] \tag{3.12}$$

$$\sigma_{22} = \sigma_{\theta\theta} = \frac{\mu_0}{2}\Big[\frac{2r}{r'R\gamma} + \frac{25r'r\gamma}{R} - 27\Big] \tag{3.13}$$

$$\sigma_{33} = \sigma_{zz} = \frac{\mu_0}{2}\Big[\frac{2R\gamma}{r'r} + \frac{25r'r\gamma}{R} - 27\Big] \tag{3.14}$$

$$\sigma_{r\theta} = \sigma_{\theta r} = \sigma_{\theta z} = \sigma_{z\theta} = \sigma_{rz} = \sigma_{zr} = 0 \tag{3.15}$$

3.2.4 EQUILIBRIUM EQUATIONS FOR DEFORMATION OF CYLINDRICAL MATERIAL

The equilibrium equations for cylindrical polar coordinates are given by ;

$$\frac{\partial\sigma_{rr}}{\partial r} + \frac{1}{r}\frac{\partial\sigma_{r\theta}}{\partial\theta} + \frac{\partial\sigma_{rz}}{\partial z} + \frac{1}{r}(\sigma_{rr} - \sigma_{\theta\theta}) = 0 \tag{3.16}$$

$$\frac{\partial \sigma_{\theta r}}{\partial r} + \frac{1}{r}\frac{\partial \sigma_{\theta\theta}}{\partial \theta} + \frac{\partial \sigma_{\theta z}}{\partial \theta} + \frac{2}{r}\sigma_{\theta r} = 0 \tag{3.17}$$

$$\frac{\partial \sigma_{zr}}{\partial r} + \frac{1}{r}\frac{\partial \sigma_{z\theta}}{\partial \theta} + \frac{\partial \sigma_{zz}}{\partial r} + \frac{1}{r}\sigma_{zr} = 0 \tag{3.18}$$

Recall the Cauchy first law of continuum mechanics where there is equilibrium and no body force;

$$\sigma_{r\theta} = \sigma_{rz} = \sigma_{\theta r} = \sigma_{\theta z} = \sigma_{rz} = \sigma_{zr} = \sigma_{z\theta} = \sigma_{zr} = 0. \tag{3.19}$$

Therefore, equations(3.16) becomes;

$$\frac{d\sigma_{rr}}{dr} + \frac{1}{r}\Big[\sigma_{rr} - \sigma_{\theta\theta}\Big] = 0, \tag{3.20}$$

$$\frac{d\sigma_{rr}}{dR} + \frac{r'}{r}\Big[\sigma_{rr} - \sigma_{\theta\theta}\Big] = 0, \tag{3.21}$$

Applying equations (3.12), (3.13) and (3.14) into equation (3.21), we obtain the model equation of cylindrical symmetric deformation with its boundary conditions as;

$$\sigma_{rr} = \frac{\mu_0}{2}\Big[\frac{2r'}{r\gamma}R + \frac{25r'\gamma}{R}r - 27\Big] \tag{3.12}$$

$$\sigma_{\theta\theta} = \frac{\mu_0}{2}\Big[\frac{2r}{r'R\gamma} + \frac{25r'r\gamma}{R} - 27\Big] \tag{3.13}$$

$$\frac{d(\mu(\frac{r'R}{r\gamma} + \frac{25r'r\gamma}{R} - 27)}{dR} + \mu\frac{2r'}{r}\Big[\frac{r'R}{r\gamma} + \frac{2r'r\gamma}{R} - 27 - (\frac{1}{r'} - \frac{2r'r\gamma}{R} - 27)\Big] = 0, \tag{3.22}$$

Note that $\mu \neq 0$ Therefore, equation (3.22) becomes;

$$\frac{d(\mu(\frac{r'R}{r\gamma} + \frac{25r'r\gamma}{R} - 27)}{dR} + \mu\frac{2r'}{r}\Big[\frac{2}{R\gamma} - \frac{2R\gamma}{r^2}\Big] = 0, \tag{3.23}$$

By simplification, equation (3.23) becomes;

$$\frac{2rR\gamma'' + 2rr' - 2R\gamma r'^2}{r^2\gamma^2} + \frac{25rR\gamma r'' + 25R\gamma r'^2 - 25r\gamma r'}{r^2\gamma^2} + \Big[\frac{2}{R\gamma} - \frac{2R\gamma}{r^2}\Big] = 0, \tag{3.24}$$

$$(2R^3 + 25r^2R\gamma^2)\frac{d^2r}{dR^2} + 25r\gamma^2R(\frac{dr}{dR})^2 - (2R^2 - 25r^2\gamma^2)\frac{dr}{dR} - 2rR = 0 \tag{3.25}$$

3.2.5 BOUNDARY VALUE MODEL EQUATION OF CYLINDRICALLY SYMMETRIC DEFORMATION

Here again, we consider a hollow cylinder of Levinson-Burgess material deforming under internal pressure of magnitude ρ acting everywhere in the inner surface such that the outer surface of the cylinder is stress free. For this deformation, the boundary conditions are:

$$(\sigma_{rr})_{R=a} = -\rho \; (\sigma_{rr})_{R=b} = 0$$

Applying the conditions of a hollow cylinder on the radial stress, we obtain the boundary conditions as;

$$(\sigma_{rr})_{R=a} = -\rho$$

$$(\sigma_{rr})_{R=a} = \frac{\mu}{2}\Big[\frac{2r'}{r\gamma}a + \frac{25r'\gamma}{a}r - 27\Big] = -\rho \tag{3.26}$$

$$r'(a) = \frac{r(a)\gamma(27 - \frac{2\rho}{\mu})}{2a^2 + 25r^2(a)\gamma^2} \tag{3.27}$$

$$(\sigma_{rr})_{R=b} = 0$$

$$(\sigma_{rr})_{R=b} = \frac{\mu}{2}\Big[\frac{2r'}{r\gamma}b + \frac{25r'\gamma}{b}r - 27\Big] = 0 \tag{3.28}$$

$$(\sigma_{rr})_{R=b} = 0 \implies r'(b) = \frac{27br(b)\gamma}{2b^2 + 25r^2(b)\gamma^2} \tag{3.29}$$

At any cross-section of the cylinder, hence we are set to solve the boundary value problem;

$$(2R^3 + 25r^2R\gamma^2)\frac{d^2r}{dR^2} + 25r\gamma^2R(\frac{dr}{dR})^2 - (2R^2 - 25r^2\gamma^2)\frac{dr}{dR} - 2rR = 0 \tag{3.25}$$

$$r'(a) = \frac{r(a)\gamma(27 - \frac{2\rho}{\mu})}{2a^2 + 25r^2(a)\gamma^2} \tag{3.27}$$

$$r'(b) = \frac{27br(b)\gamma}{2b^2 + 25r^2(b)\gamma^2} \tag{3.29}$$

Chapter 4

RESULTS AND DISCUSSION

4.1 SOLUTIONS FOR SPHERICAL AND CYLINDRICAL SYMMETRIC DEFORMATION

We now proceed to investigate the displacements and stresses of the compressible rubber-like material undergoing internal pressure. First, we consider the derived equation of spherically and cylindrically symmetric deformations which we solved numerically by the help of Mathematica(ode45 solver) and collocation. The boundary value problem is a second-order nonlinear ordinary differential equations which at this moment has no analytical solution even after applying several techniques. The load applied is the same at every height and the load considered here is the pressure which is applied at a constant rate at the inner surface. This load applied generates stresses within the cylinder and the outer surface is stress free. In this chapter, we are set to solve two boundary value problems

$$(2R^4 + 25r^4R)\frac{d^2r}{dR^2} + 50r^3R(\frac{dr}{dR})^2 + (4R^3 - 50r^4)\frac{dr}{dR} - 2rR^3 = 0 \tag{3.32}$$

$$r'(a) = \frac{a^2 r^2(a)(27\mu_0 - 2\rho)}{\mu_0(2a^4 + 25r^4(a))} \tag{3.33}$$

$$r'(b) = \frac{27b^2 r^2(b)}{2b^4 + 25r^4(b)} \tag{3.35}$$

$$(2R^3 + 25r^2 R\gamma^2)\frac{d^2 r}{dR^2} + 25r\gamma^2 R(\frac{dr}{dR})^2 - (2R^2 - 25r^2\gamma^2)\frac{dr}{dR} - 2rR = 0 \tag{3.25}$$

$$r'(a) = \frac{r(a)\gamma(27 - \frac{2\rho}{\mu})}{2a^2 + 25r^2(a)\gamma^2} \tag{3.27}$$

$$r'(b) = \frac{27br(b)\gamma}{2b^2 + 25r^2(b)\gamma^2} \tag{3.29}$$

for the spherical hollow and cylindrical hollow materials composed of the same strain energy density function;

$$W = \frac{\mu_0}{2}\left[I_1 - 27\sqrt{I_3} + \frac{25}{2}I_3 + \frac{23}{2}\right] \tag{2.6}$$

The two sets of equation above are highly nonlinear second order ordinary differential equation. Every effort made to solve these equation analytically proved abortive, hence, we resorted to numerical methods of solution. Solving these problems using two methods; shooting method and collocation methods into Mathematica, we were able to obtain the following results.

4.1.1 COLLOCATION METHOD FOR NONLINEAR SECOND-ORDER BOUNDARY VALUE PROBLEMS

Exponentially fitted backward differentiation scheme for general second order differential equations derived via collocation method, with frequency $w = 1$, $\gamma = 1.0315$, $h = \frac{(b-a)}{N}$; where (a,b) is the interval of integration, N is number of subintervals and $a = x_0 < x_1 < .... < x_N = b$.

$$y_{2+i} = \frac{1}{((-1+e^{hw})^2 w^2)}(f_i - 2e^{hw}f_i + e^{2hw}f_i - e^{hw}h^2w^2f_i - 2f_{1+i} + 4e^{hw}f_{1+i} - 2e^{2hw}f_{1+i} +$$

$$h^2w^2f_{1+i} + e^{2hw}h^2w^2f_{1+i} + f_{2+i} - 2e^{hw}f_{2+i} + e^{2hw}f_{2+i} - e^{hw}h^2w^2f_{2+i} - w^2y_i + 2e^{hw}w^2y_i -$$

$$e^{2hw}w^2y_i + 2w^2y_{1+i} - 4e^{hw}w^2y_{1+i} + 2e^{2hw}w^2y_{1+i})$$

$$yp_i = \frac{-1}{6(-1+e^{hw})^2hw^2}(-6f_i] + 6e^{hw}f_i - 6f_i - 5e^{hw}h^2w^2f_i + 2^{2hw}h^2w^2f_i + 12f_{1+i} - 12e^{hw}f_{1+i} +$$

$$12hwf_{1+i} + 5h^2w^2f_{1+i]} + e^{2hw}h^2w^2f_{1+i} - 6f_{2+i} + 6e^{hw}f_{2+i} - 6hwf_{2+i} - 2h^2w^2f_{2+i} -$$

$$e^{hw}h^2w^2f_{2+i} + 6w^2y_i - 12e^{hw}w^2y_i + 6e^{2hw}w^2y_i - 6w^2y_{1+i} + 12e^{hw}w^2y_{1+i} - 6e^{2hw}w^2y_{1+i})$$

$$yp_{1+i} = \frac{1}{6(-1+e^{hw})^2hw^2}(6f_i - 6e^{hw}f_i + 6e^{hw}hwf_i - 4e^{hw}h^2w^2f_i + e^{2hw}h^2w^2f_i - 12f_{1+i} + 12ehwf_{1+i} -$$

$$12e^{hw}hwf_{1+i} + 4h^2w^2f_{1+i} + 2e^{2hw}h^2w^2f_{1+i} + 6f_{2+i} - 6e^{hw}f_{2+i} + 6e^{hw}hwf_{2+i} - h^2w^2f_{2+i} -$$

$$2e^{hw}h^2w^2f_{2+i} - 6w^2y_i + 12e^{hw}w^2y_i - 6e^2hww^2y_i + 6w^2y_{1+i} - 12e^{hw}w^2y_{1+i} + 6e^{2hw}w^2y_{1+i})$$

$$yp_{2+i} =$$

$$\frac{-1}{6(-1+e^{hw})^2hw^2}(-6f_i + 6e^{hw}f_i - 6e^{2hw}hwf_i + 7e^{hw}h^2w^2f_i + 2e^{2hw}h^2w^2f_i + 12f_{1+i} - 12e^{hw}f_{1+i} +$$

$$12e^{2hw}hwf_{1+i} - 7h^2w^2f_{1+i} - 11e^{2hw}h^2w^2f_{1+i} - 6f_{2+i} + 6E^{hw}f_{2+i} - 6e^{2hw}hwf_{2+i} - 2h^2w^2f_{2+i} +$$

$$11e^{hw}h^2w^2f_{2+i} + 6w^2y_i - 12e^{hw}w^2y_i + 6e^{2hw}w^2y_i - 6w^2y_{1+i} + 12e^{hw}w^2y_{1+i} - 6e^{2hw}w^2y_{1+i}$$

Below are the results of the second order nonlinear ordinary differential equation:

Table 4.1: Table for shooting method Versus Collocation method from (3.32) (N= 20)

R	r(R)(shooting method)	r(R) derived method	σ_{rr}(shooting/derived method)
0.20	0.01501	0.01501	-0.4974
0.24	0.01746	0.01746	-1.5854
0.28	0.01933	0.01933	-2.2169
0.32	0.02084	0.02084	-2.4283
0.36	0.02217	0.02217	-2.3692
0.40	0.02339	0.02339	-2.2152
0.44	0.02455	0.02455	-2.0456
0.48	0.02565	0.02565	-1.8763
0.52	0.02670	0.02670	-1.7081
0.56	0.02772	0.02772	-1.5463/-1.5429
0.6	0.02869	0.02869	-1.3846/-1.3812
0.64	0.02963	0.02963	-1.2307
0.68	0.03055	0.03055	-1.0819
0.72	0.03144	0.03143	-0.9362/-0.9362
0.76	0.03230	0.03229	0.7929
0.8	0.03314	0.03313	-0.6529/-0.6495
0.84	0.03396	0.03395	-0.5163/-0.5130
0.88	0.03476	0.03475	-0.3841
0.92	0.03554	0.03553	-0.2546/-0.2512
0.96	0.03630	0.03630	-0.1228
1.	0.03705	0.03705	-0.00035

Figure 4.1: spherically symmetric deformation from (3.32) for N = 20

Graphical representation of the solution at N = 20

```
Plot[Evaluate[r[R] /. sols], {R, 0.2, 1}, AxesLabel -> {"R", "r(R)"}]
```

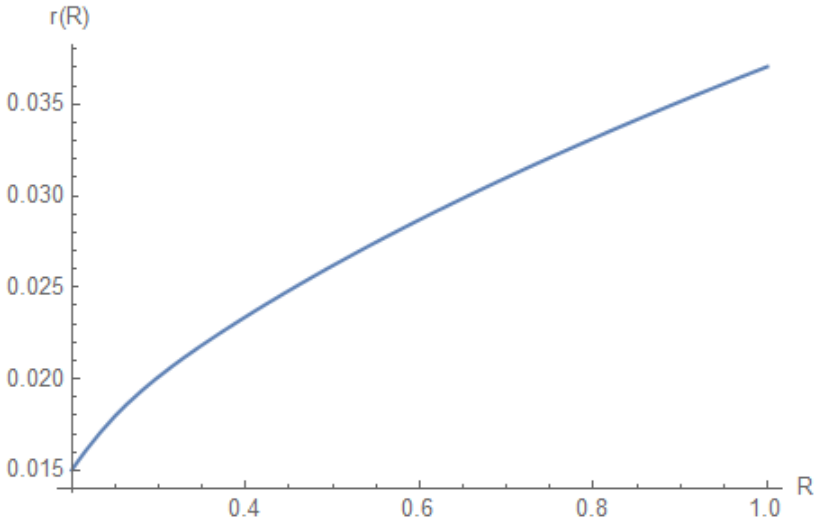

This is the graph for $N = 20$ from (3.32). Result shows that for the shooting method, $r(0.2) = 0.01501m$ and $r(1) = 0.03705$. This means that there is steady increase in the deformation of the material at maximum load of $\rho = 0.5N/m^2$ .Increase in pressure will blow up the material.

Figure 4.2: spherically symmetric deformation Versus Collocation method for N = 20

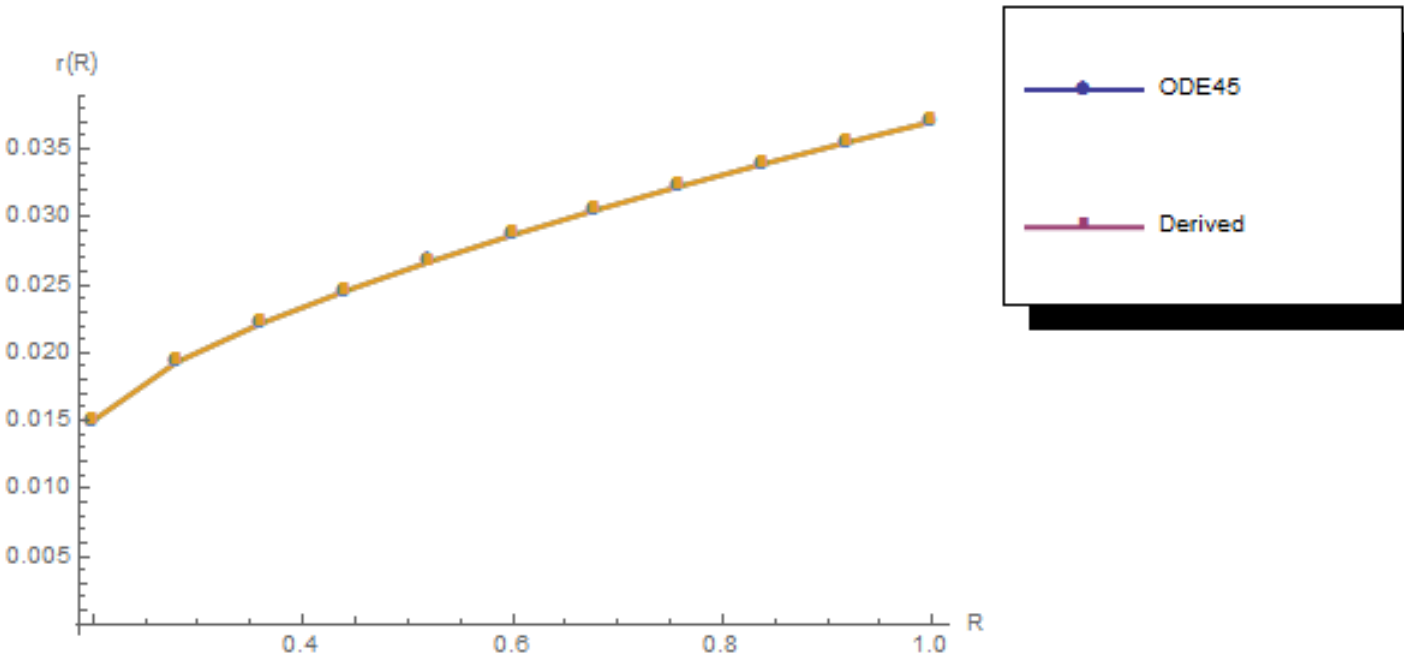

This is the graph for $N = 20$ from (3.32) showing the simulation of Collocation(Derived) and Shooting method(ODE45). Result shows that the displacements of both methods are $r(0.2) = 0.01501m$ and $r(1) = 0.03705m$. This means that there is steady increase in the deformation of the material at maximum load of $\rho = 0.5N/m^2$ .Increase in pressure will blow up the material.

Table 4.2: Table for shooting method versus Collocation method (3.32) (N= 40)

R	r(R)(shooting method)	r(R) Derived method	σ_{rr}(shooting/derived method)
0.20	0.01501	0.01501	-0.4974
0.22	0.01632	0.01632	-1.1023
0.24	0.01746	0.01746	-1.5854
0.26	0.01846	0.01846	-1.9600
0.28	0.01933	0.01933	-2.2169
0.30	0.02012	0.02012	-2.2169
0.32	0.02084	0.02084	-2.4283
0.34	0.02152	0.02152	-2.4189
0.36	0.02217	0.02217	-2.3692
0.38	0.02279	0.02279	-2.2972
0.4	0.02339	0.02339	-2.2152
0.42	0.02398	0.02398	-2.1314
0.44	0.02455	0.02455	-2.0456
0.46	0.02511	0.02510	-1.9626/-1.9593
0.48	0.02565	0.02565	-1.8763
0.50	0.02618	0.02618	-1.7918
0.52	0.02670	0.02670	-1.7081
0.54	0.02721	0.02721	-1.6260
0.56	0.02772	0.02771	-1.5463/-1.5429
0.58	0.02821	0.02820	-1.4651/-1.4617
0.60	0.02870	0.02869	-1.3846/-1.3812
0.62	0.02917	0.02916	-1.3095/-1.3062
0.64	0.02963	0.02963	1.2307
0.66	0.03009	0.03009	-1.550
0.68	0.03055	0.03055	-1.0819
0.70	0.03099	0.03099	-1.0065
0.72	0.03144	0.03143	-0.9362
0.74	0.03187	0.03187	-0.8628
0.76	0.03230	0.03229	-0.7929
0.78	0.03272	0.03272	-0.7202
0.8	0.03314	0.03313	-0.6529/-0.6495
0.82	0.03355	0.03355	-0.5849
0.84	0.03396	0.03395	-0.5163
0.86	0.03436	0.03436	-0.4493
0.88	0.03476	0.03475	-0.3841
0.90	0.03515	0.03515	-0.3171
0.92	0.03554	0.03553	-0.2546/-0.2512
0.94	0.03592	0.03592	-0.1866
0.96	0.03630	0.03630	-0.1228
0.98	0.03668	0.03668	-0.0629
1.00	0.03705	0.03705	-0.00035

Figure 4.3: spherically symmetric deformation for N = 40

Graphical representation of the solution

```
Plot[Evaluate[r[R] /. sols], {R, 0.2, 1}, AxesLabel -> {"R", "r(R)"}]
```

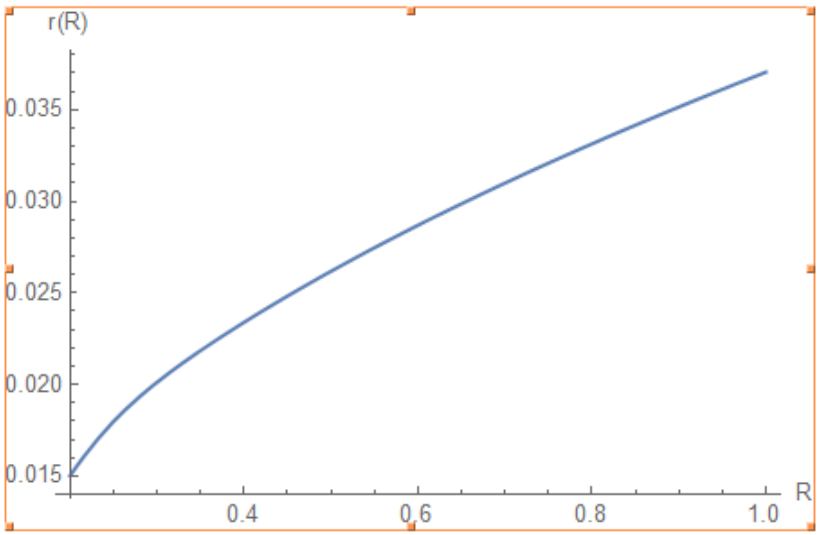

For $N = 40$ from (3.32), Result shows that for the shooting method, $r(0.2) = 0.01501m$ and $r(1) = 0.03705$. This means that there is steady increase in the deformation of the material at maximum load of $\rho = 0.5N/m^2$ .Increase in pressure will blow up the material.

Figure 4.4: spherically symmetric deformation Versus Collocation method for N = 40

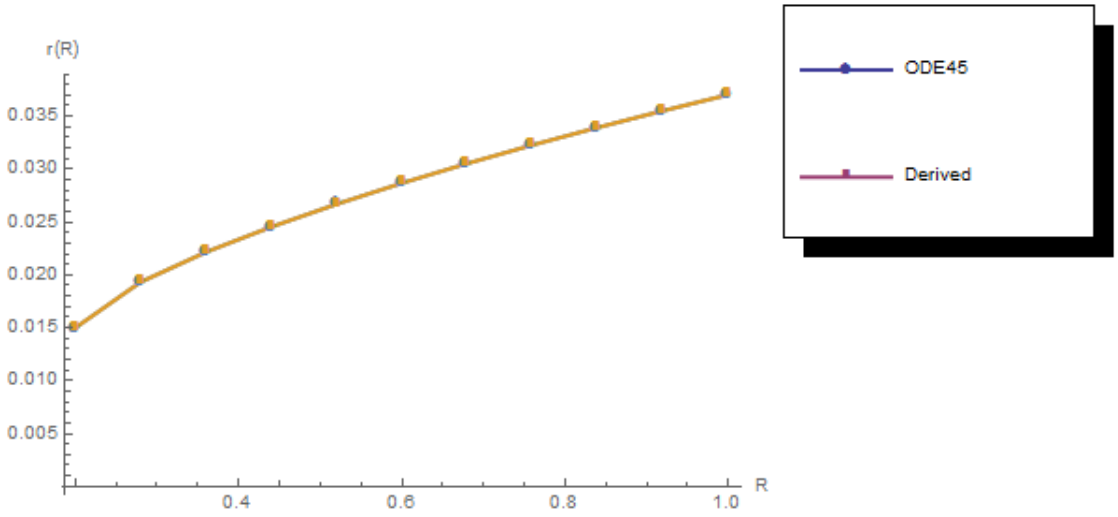

The graph for $N = 40$ from (3.32) showing the simulation of Collocation(Derived) and Shooting method(ODE45). Result shows that the displacements of both methods are $r(0.2) = 0.01501m$ and $r(1) = 0.03705m$. This means that there is steady increase in the deformation of the material at maximum load of $\rho = 0.5N/m^2$ .Increase in pressure will blow up the material.

Table 4.3: Table for shooting method Versus Collocation(Derived) method from (3.25) (N= 20)

R	r(R)(shooting method)	r(R) Derived method	σ_{rr}(shooting/derived method)
0.20	0.39735	0.39731	8.7399/8.7384
0.24	0.44572	0.44567	7.0302/7.0288
0.28	0.49167	0.49163	6.9852/6.9839
0.32	0.53575	0.53570	4.8205/4.8196
0.36	0.57832	0.57826	4.0632/4.0622
0.40	0.61964	0.61958	3.4486/3.4477
0.44	0.65992	0.65986	2.5117/2.5109
0.48	0.69932	0.69925	2.5117/2.5109
0.52	0.73794	0.73787	2.1463/2.1455
0.56	0.77591	0.77583	1.8309/1.8302
0.60	0.81330	0.81321	1.5562/1.5553
0.64	0.85017	0.85009	1.3144/1.3137
0.68	0.88659	0.88650	1.1004/1.0097
0.72	0.92261	0.92252	0.9096/0.9089
0.76	0.95827	0.95817	0.7387/0.7380
0.80	0.99360	0.99350	0.5846/0.5840
0.84	1.02864	1.02853	0.4452/0.4445
0.88	1.06341	1.06330	0.3184/0.3178
0.92	1.09794	1.09783	0.2029/0.2023
0.96	1.13226	1.13215	0.0971/0.0965
1.00	1.16638	1.16626	-1.2973e-05/-5.8495e-04

Figure 4.5: cylindrically symmetric deformation from (3.25) for N = 20

Graphical representation of the solution

```
Plot[Evaluate[r[R] /. sols], {R, 0.2, 1}, PlotStyle → {Thick}]
```

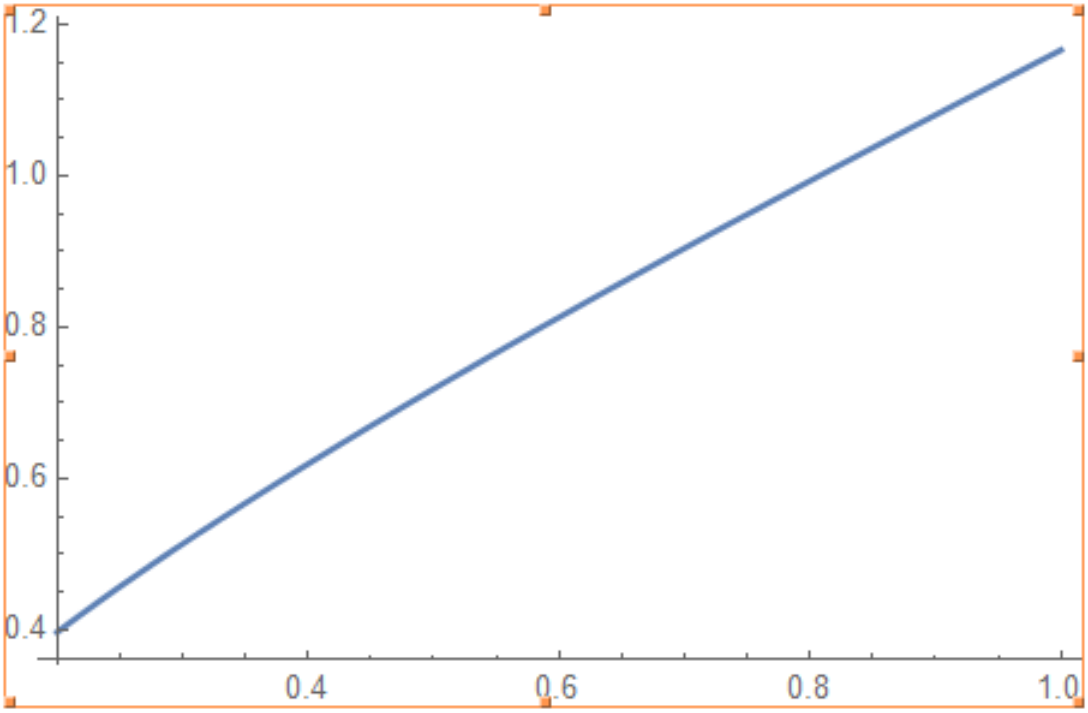

For $N = 20$, the graph above describes the cylindrical deformation of the nonlinear ODE of (3.25) using shooting method on Mathematica at $r(0.2) = 0.39735m$ and $r(1) = 1.16638m$ when maximum $\rho = 14N/m^2$. There is steady increase in displacements when the pressure increases. The material will blow up when it exceeds the maximum pressure. This is also true for figure 4.6.

Figure 4.6: cylindrical(shooting method) and Collocation method for N = 20

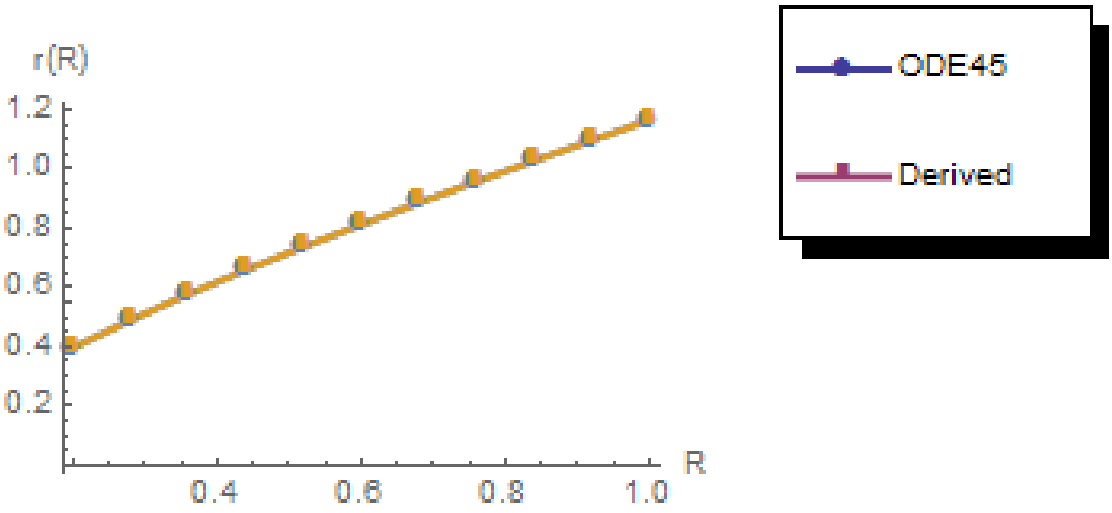

Table 4.4: Table for cylindrical shooting method Versus Collocation method from (3.25) (N= 40)

R	r(R)(shooting method)	r(R) Derived method	σ_{rr}(shooting/derived method)
0.20	0.39735	0.39731	8.7399/8.7384
0.22	0.42188	0.42184	7.8131/7.8118
0.24	0.44572	0.44567	7.0302/7.0288
0.26	0.46896	0.46891	6.3595/6.3583
0.28	0.49167	0.49162	6.9852/9839
0.30	0.51392	0.51387	5.2697/5.2686
0.32	0.53575	0.53570	4.8205/4.8196
0.34	0.5572	0.55715	4.4209/4.4200
0.36	0.57832	0.57826	4.0632/4.0622
0.38	0.59912	0.59907	3.7406/3.7398
0.40	0.61964	0.61958	3.4486/3.4477
0.42	0.63990	0.63984	3.1827/3.1819
0.44	0.65992	0.65986	2.9398/2.9391
0.46	0.67972	0.67965	2.7170/2.7161
0.48	0.69932	0.69925	2.5117/2.5109
0.50	0.71872	0.71865	2.3220/2.3212
0.52	0.73794	0.73787	2.1463/2.1455
0.54	0.75700	0.75693	1.9829/1.9822
0.56	0.77591	0.77583	1.8309/1.8302
0.58	0.79467	0.79459	1.6889/1.6882
0.60	0.81330	0.81321	1.5562/1.5553
0.62	0.83179	0.83171	1.4314/1.4307
0.64	0.85017	0.85009	1.3144/1.3137
0.66	0.86843	0.86835	1.1620/1.1613
0.68	0.88659	0.88650	1.1004/1.0097
0.70	0.90465	0.90456	1.0023/1.0016
0.72	0.92261	0.92252	0.9096/0.9089
0.74	0.94048	0.94039	0.8218/0.8212
0.76	0.95827	0.95817	0.7387/0.7380
0.78	0.97597	0.97587	0.6596/0.6590
0.80	0.99360	0.99350	0.5846/0.5840
0.82	1.01115	1.01105	0.4871/0.4866
0.84	1.02864	1.02853	0.4452/0.4445
0.86	1.04605	1.04595	0.3803/0.3797
0.88	1.06341	1.06330	0.3184/0.3178
0.90	1.08070	1.08060	0.2593/0.2588
0.92	1.09794	1.09783	0.2029/0.2023
0.94	1.11513	1.11502	0.1488/0.1482
0.96	1.13226	1.13215	0.0971/0.0965
0.98	1.14934	1.14923	0.0475/0.0470
1.00	1.16638	1.166263	-1.2973e-05/-5.8495e-04

Figure 4.7: cylindrically symmetric deformation for N = 40

Graphical representation of the solution

```
Plot[Evaluate[r[R] /. sols], {R, 0.2, 1}, PlotStyle → {Thick}]
```

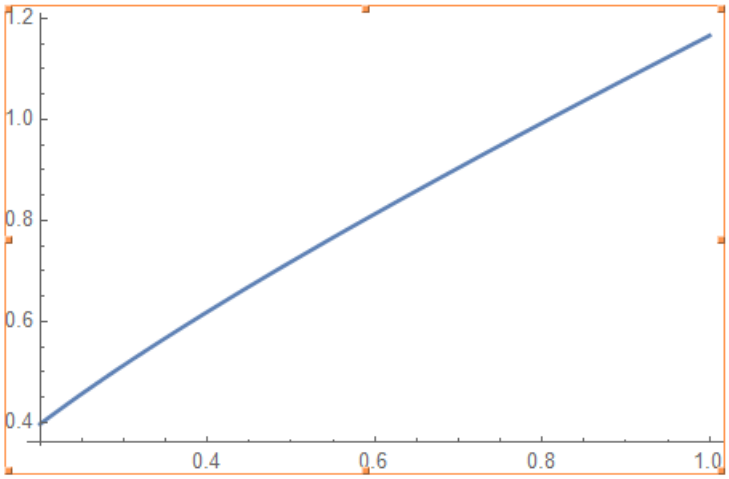

For $N = 40$, the graph above describes the cylindrical deformation of the nonlinear ODE of (3.25) using shooting method on Mathematica at $r(0.2) = 0.39735m$ and $r(1) = 1.16638m$ when maximum $\rho = 14N/m^2$. There is steady increase in displacements when the pressure increases. The material will blow up when it exceeds the maximum pressure. This is true for figure 4.8 which shows the graph of the two methods for validation of our results. The difference between figures 4.6 and 4.8 is simply the number of iterations which is N = 20 and N = 40 respectively.

Figure 4.8: cylindrical(shooting method) and Collocation method for N = 40

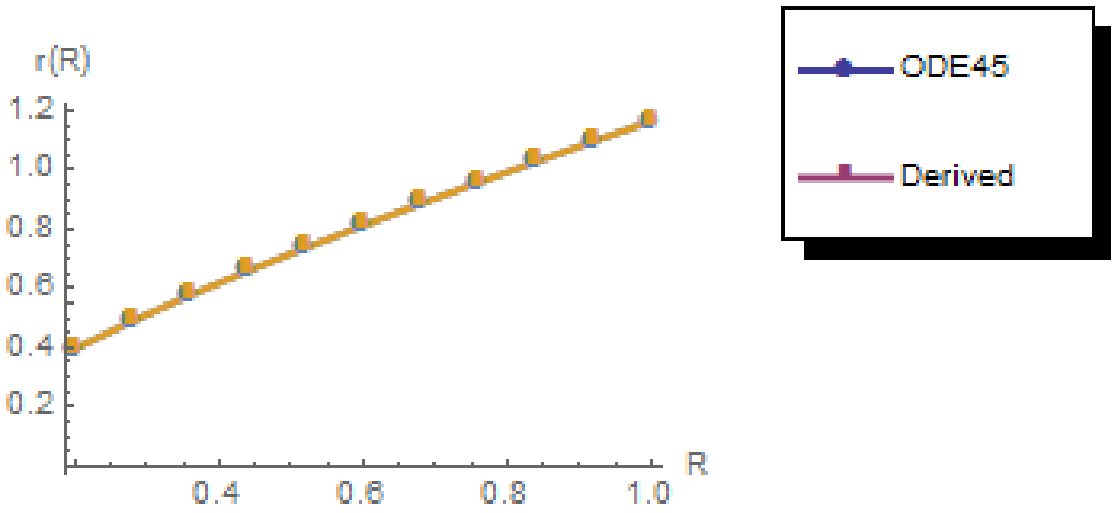

Figure 4.9: Graph for r'(R) Versus R

Graphical representation of the solution

```
Plot[Evaluate[r'[R] /. sols], {R, 0.2, 1}, AxesLabel -> {"R", "r'(R)"}]
```

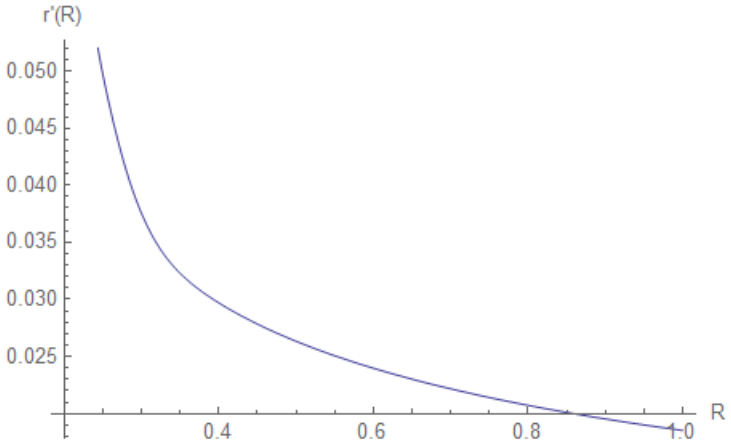

Figures 4.9 and 4.10 are the plots of the gradient against the radius R. The $r'(R)$ helped us to obtain the stresses acting on the material. At $R = 0.2m$, the gradient $r'(R) = 1.24m$ for the cylindrical deformation which serves as their point of interception while at $r'(R) = 0.2m$, $R = 0.82m$ for the Spherical deformation. This shows changes on the materials as regards the stresses. Figures (4.9) and (4.10) show that $r'(R)$ is decreasing and both are said to be concave down. They are also less steep. Figure (4.9) has a vertical asymptote at $R = (0.2, 1)$ while figure (4.10) has a horizontal asymptote at $R = (0.2, 1)$. Note that the radius of a circle, a sphere or cylinder and any other shape with circular surface on it is a measurement. For us to have obtained a negative radius, it shows that there is more than one center and at this point, the circumference becomes the center.

Figure 4.10: Graph for r'(R) Versus R

Graphical representation of the solution

```
Plot[Evaluate[r'[R] /. sols], {R, 0.2, 1},
 AxesLabel → {"R", "r'(R)"}]
```

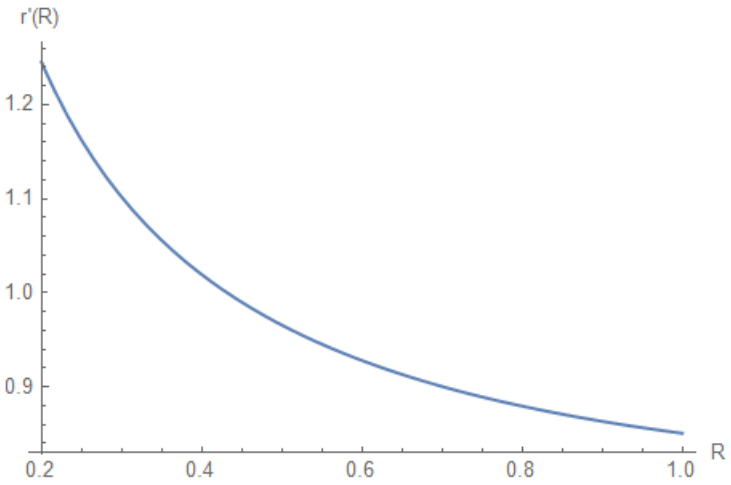

4.1.2 STATISTICAL ANALYSIS USING T-TEST

Considering the table of solution for spherical coordinates;

for table 4.1:

p-value is 0.2878

p-value summary shows not significant

significantly different($p < 0.05$)? No

t, df = (t = 1.092, df = 20)

number of pairs is 21

mean of difference is 0.0003865

Standard deviation difference is 0.001652

95 percent confidence interval is -0.0003653 to 0.001138.

for table 4.2:

p-value is 0.3306

p-value summary shows not significant

significantly different($p < 0.005$)? No

t, df = (t = 0.9848, df = 40)

number of pairs is 41

mean of difference is 0.0001820

Standard deviation of difference is 0.001183

95 percent confidence interval is -0.0001914 to 0.0005553.

Considering the table of solution for cylindrical coordinates;

for table 4.3:

$p - value < 0.0001$

p-value summary shows it is significant

significantly different($p < 0.005$)? Yes

t, df = (t = 15.60, df = 20)

number of pairs is 21

mean of difference is -8.026e-005

Standard deviation of difference is 2.357e-005

95 percent confidence interval is -9.099e-005 to -6.953e-005.

for table 4.4:

$p - value < 0.0001$

p-value summary shows it is significant

significantly different($p < 0.005$)? Yes

t, df = (t = 22.63, df = 40)

number of pairs is 41

mean of difference is -8.026e-005

Standard deviation of difference is 2.272e-005

95 percent confidence interval is -98.749e-005 to -7.314e-005.

4.1.3 ANALYSIS OF RESULTS

Different graphs were plotted each for both the spherical and cylindrical deformations at $N = 20$ and $N = 40$ respectively. For Spherical deformation, in figure (4.1) and figure(4.2), we obtained same values for$r(R)$ for both methods. At $N = 20$, we obtained same values for their corresponding stresses except for $R = (0.56m, 0.6m, 0.72m, 0.8m, and0.92m)$ while we have $R = (0.46, 0.56, 0.58, 0.60, 0.62, 0.8and0.92f)$. $r(0.2) = 0.01501m$ and $r(1) = 0.03705m$ are boundary conditions which have corresponding stresses acting at the respective points at $\sigma(r(0.2)) = -0.4974kg/m/s^2$ and $\sigma(r(1)) = -0.00035kg/m/s^2$. The graph above shows that as the pressure increases, the stress acting on the body also increases. figure (4.2) is a comparison of both shooting and collocation methods. From the statistical results as presented above, there is no significant difference(for tables 4.1 and 4.2) between the shooting method and the collocation method. This implies that the two methods are the same since the p-value is greater than 0.005. Similarly, the displacements for the cylindrical deformation at $r(a)$ and $r(b)$ are $r(0.2) = 0.39735m$ and $r(1) = 1.16638m$ and corressponding stresses of $\sigma(r(0.2)) = 8.7399kg/m/s^2$ and $\sigma(r(1)) = -1.2973e - 05kg/m/s^2$ for the shooting method and for the collocation method we obtained $r(0.2) = 0.39731m$ and $r(1) = 1.16626m$ with stresses $\sigma(r(0.2)) = 8.7384kg/m/s^2$ and $\sigma(r(1)) = 5.849e - 04kg/m/s^2$.. It is found that as the pressure increases, the stress acting on the material also increases. There are significant variations in the stresses and even at different points of radius. The results apply for $N = 20$ and$N = 40$.

If the pressure increases beyond that, the material inflates, reaches a amximum with value $r(1) = 1.16626m$. The table compares the solution as obtained using shooting method internally in mathematica(ode45 solver) and the derived collocation method applied to obtain the results for

displacements. In the case of tables 4.3 and 4.4, we observed there is no significant difference as we obtained a p-value less than 0.0001 which is much less than the prescribed 0.005.

It is well known that the displacement equations of equilibrium in finite elastostatics may lose ellipticity at sufficiently large deformations. For $\rho = 0.5N/m^2$ the maximum load is obtained for the spherical deformation $\rho = 14N/m^2$ for cylindrical deformation respectively before loss of ellipticity occurs. The existence of smooth solution is obtained after loss ellipticity. Moreover, the possibilty exists that non-smooth deformation fields with discontinuous deformation gradients and stresses might occur. This can be compared with the arguement shown in Chung et al(1986) where they deduced that as the pressure, ρ, is increased, the deformed radius increases until ρ reaches a maximum value where $r(1) = 0.03705$. Our results is in agreement with this work by Chung et al(1986) who also showed that axisymmetric solutions with discontinuities do not exist in their work. If Weak solution exists, then it must be non-axisymmetric.

Chapter 5

CONCLUSION AND RECOMMENDATION

The result was applied to the determination of stresses and displacement in the radial deformation which was solved numerically at maximum pressures by the help of Mathematica (ode45 solver) algorithm which used shooting method internally and we validated the shooting method with our derived results, where we applied collocation method to solve for both spherical and cylindrical problems. The argument posed by Chung et al(1986)is that as the pressure(ρ) increases, the deformed radius increases until ρ reaches its maximum value where $r(a) = 1$. This arguments holds for both the spherical and cylindrical deformations.

In our work, axisymetric solutions with discontinuities do not exist. If weak solution exist, they must be axisymmetric. As the pressure increases, the material inflates. Our results show that the cylindrical symmetric deformation attains its maximum pressure at $\rho = 14N/m^2$ and when for example, the material is inflated too much, the rubber rounds out at the top of the material will quickly wear out. There will be traction reduction which is responsible for the material to burst . Again, the spherically symmetric deformation has its maximum pressure at $\rho = 0.5N/m^2$ and

anything more than that blows up the system and the solution diverges. From the table and graphical simulations, the result from shooting method for spherical deformations agree with the result from our derived collocation method for the same boundary value problems. But that of cylindrical deformation has significant difference and as such, the two methods did not agree even though they are only slightly different. We also discovered that increase in mesh points guarantees finer results. This research work on finite deformations of internally pressurizedisotropic compressible synthetic rubber-like material.The type of load considered for a material that has Levinson-Burgess strain energy function is used because most strain energy functions are particular form of this strain energy function. Several methods of analytical approach to solve the resulting boundary value problem was sort but no solution was obtained at the moment. Fortunately, a lot of software have been developed to handle such highly nonlinear second order ordinary differential equations with specific values of parameters. We were able to determine the stresses and displacements of the resultant second order nonlinear ordinary differential equation with its boundary conditions for both the spherical and cylindrical materials. This research work can be applied to the problem of radial tyre under internal pressure. .

From the t-test, we can say that both methods have the same results for the spherical symmetric deformation because the p-value has no significant difference. However, the p-value is significant for the cylindrical symmetric deformation and this means that the solution with smaller values when compared give a better result. Collocation method is therefore a better method from our statistical analysis.

5.0.1 CONTRIBUTION TO KNOWLEDGE

- In our work, we were able to determine the general equation for the pressure (ρ) in a general material composed of Levinson-Burgess strain energy function, which hitherto had been avoided by other authors.

- We were able to develop numerical schemes using shooting and Collocation methods which makes it easy to determine position of maximum stresses and pressure in a spherical and cylindrical material of Levinson-Burgess strain energy function. These numerical schemes can solve any nonlinear second-order ordinary differential equations with any given boundary conditions on Mathematica Software.

5.0.2 RECOMMENDATION

- We recommend that the strain energy function of Levinson and Burgess be compared with the strain energy functions of other rubber-like materials such as Neo-Hookean, Mooney-Rivlin and other using the same boundary conditions for the determination of the behaviour of the materials.

- Finite element method can be applied on Matlab for an improved result especially when considering the displacement distribution and stresses acting on a tyre when in contact with the ground under internal pressure.

- Since we have not been able to get the analytical solution, closed form solution of the nonlinear second-order ordinary differential equations obtained by analytical methods will make a huge contribution to knowledge.

REFERENCES

Aani, Y. & Rahimi, G.H.(2015). Stress analysis of thick pressure vessel composed of functionally graded incompressible hyperelastic materials, *International Journal of Mechanical Sciences*, 104 , 1-7.

Aani, Y. & Rahimi, G.H.(2018). On the stability of internally pressurized thick-walled spherical and cylindrical shells made of functionally graded incompressible hyperelastic material. *Latin American Journal of Solids and Structures*, 15(4).

Aani, Y. & Rahimi, G.H.(2015). Stress analysis of thick pressure vessel composed of incompressible hyperelastic materials, *International Journal of Recent Advances in Mechanical Engineering*, 4(3) ,19-37.

Adel, T., Makrem, A., Abdelmalek, Z., Adel, H., Jale, B. & Mohammed, I.(2017). On the nonlinear viscoelastic behaviour of rubber-like materials: Constitutive description and identification. *International Journal of Mechanical Sciences*, 130, 437-447

Ahmed, G.K. & Mark, E.B.(2017). New model for hyperelastic materials behaviour with an application on natural rubber. *International Manufacturing Science and Engineering*, 1-11.

Akhundov, V.M.(2014). Modeling large deformations of fibrous bodies of revolution based on applied and carcass theories 1. Butt-End torsion of cylindrical and toroidal bodies. *Mechanics of Composite Materials*, 50(2), 245-256.

Akhundov, V.M. & Skripochka, T.A.(2011). Axisymmetric deformation of revolving cylinders made of homogeneous and fibre-reinforced elastic materials. Mechanics of

Composite Materials. *Mechanics of Composite Materials*, 47(2), 211-220.

Akhundov, V.M. & Lunev, V.P.(2013). Modeling of the forming of radial tyre carcass based on applied theory of fibre-reinforced materials. *International Polymer Science and Technology*, 40(10), 37-40.

Ali, A., Hosseini, M., & Sahari, B.B(2010). A review and comparison on some rubber elasticity models, *Journal of Scientific and Industrial Research*, 69, 495-500.

Altenbach, H. & Eremeyev, V.A.(2010). On the effective stiffness of plates made of hyperelastic materials with initial stresses. *International Journal of Non-Linear Mechanics*, 45(10), 976-981.

Alwan, H.M. & Hamza, M.N.(2010). Hyperelastic constitutive modeling of rubber and rubber-like materials under finite strain. *Engineering and Technology Journal*, 28(13), 2560-2575.

Andalaft-Chacur .A., Ali Montaz .M.& Salazar Gonzalez .J.,(2011):Real Options Pricing by the Finite Element Method. *(Elsevier) Computers and Mathematics with Applications Journal*, 61, 2863-2873.

Baker, M., & Ericksen, J.L.(1954):Inequalities restricting the form of the stress-deformation relations for isotropic elastic solids and Reiner-Rivlin fluids. *Journal of the Washington Academy of Sciences*, 44(2), 33 - 35.

Blatz, P.J. & Ko, W.L.(1962):Constitutive model in nonlinear finite element analysis. *Trans. Soc. Rheol.*,6, 223 - 251.

Blatz, P.J. & Ko, W.L.(1962): Application of finite elasticity to the deformation of rubbery materials. *Trans. Society Rheol.*, 6, 223-251

Bolzon, G. & Vitaliani(1993): The Blatz-Ko material model and homogenization. *Archive of Applied Mechanics*, 63, 228-248.

Chen, T.L. & Durelli, A.J.(1974):Displacements and Finite-Strain Fields in Hollow Sphere Subjected to Large Elastic Deformations. *International Journal of Mechanical Sciences*, 16, 777-788.

Chung, D.T., Horgan, C.O. & Abeyaratne, R.(1986). The finite deformation of internally pressurized hollow cylinders and spheres for a class of compressible elastic materials.

International Journal of Solids and Structures, 22(12), 1557-1570.

Criscione, J.C., Douglas, A.S, & Hunter, W.C.(2001): Physically based invariant set for materials exhibiting transversley isotropic behaviour. *Journal of Mechanics and Phyical Solids*, 49, 871 -897.

De Pasclis, R., Abrahams, I.D., and Parnell, W.J.(2015). Simple shear of a compressible quasilinear viscoelastic material. *International Journal of Engineering Science*, 88, 64-72.

Egbuhuzor U.P. & Erumaka E.N.(2020). Finite Deformation of Internally Pressurized Spherical Compressible Rubber-like Material. *Asian Research Journal of Mathematics*, 16(3), 38-49.

Egbuhuzor, U.P. & Eze, E.O.(2013). The Dynamic Problem for a Class of Incompressible Solids. *Int. Journal of Mathematical Research and Science(IJMRS)*, 16-20.

Ericksen, J.L.(1955): Deformations possible in every compressible , isotropic, perfectly elastic material. *Journal of mathematical physics*, 34, 126-128.

Erumaka, E. N. (2003) finite deformation of a class of Ogden solid under anti-plane shear. Journal of mathematics sciences, 14(2), 65-72.

Erumaka, E.N. (2007). Finite deformation of a rotating sphere of blatz-Ko Material. *Journal of mathematical sciences*, 18(1) ,19-24.

Erumaka, E.N. (2007). Torsion of bonded Ogden material. *Journal of mathematical sciences*, 18(1), 33-39.

Fereidoonnezhad, B., Naghdabadi, R. & Arghavani, J.(2013). A hyperelastic constitutive model for fibre-reinforced rubber-like materials. *International Journal of Engineering Science*, 71, 36-44.

Fosdick, R., Foti, P., Fraddosio, A., Marzano, S. & Piccioni, M.D.(2014). Taylor-like bifurcations for a compressible isotropic elastic tube. *Mathematics and Mechanics of Solids*, 19(8), 966-987.

Giuseppe, P. & Giuseppe, S.(2015). The Gent model for rubber-like materials: An appraisal for an ingenious and simple idea. *International Journal of Non-Linear Mechanics*, 68, 17-24.

Goncalves, P.B., Pamploma, D., & Lopes, S.R.X.(2008). Finite deformations of an initially stressed cylindrical shell under internal pressure. *International Journal of Mechanical Sciences*, 50(1), 92-103.

Guo, Z., & Sluys, L.J.(2008). Constitutive modeling of hyperelastic rubber-like materials. *HERON*, 53(3).

Hao, L., Yuyu, Z., Xiaoming, W., Zhengnam, Y. & Heng, X.(2014) Obtaining multi-axial elastic potentials for rubber-like materials via an explicit, exact approach based on spline interpolation. *Acta Mechanica Solida Sinica*, 27(5), 441-453.

Hao, D., Li, D. & Liao, Y.(2015). A finite viscoelastic constitutive model for filled rubber-like materials. *International Journal of Solids and Structures*, 64, 232-245.

Hasanpour, K., Ziaei-Rad, S., & Mahzoon, M.(2009). A large deformation framework for incompressible viscoelastic materials: Constitutive equations and finite element

implementation. *International Journal of Plasticity*, 25(6), 1154-1176.

Hill, J.M.(1992): Cylindrical and Spherical Inflation in Compressible Finite Elasticity. *IMA Journal of Applied Mathematics*, 50, 195-201.

Horgan, C.O.(1996): Remarks on ellipticity for the generalized Blatz-Ko constitutive model for compressible nonlinearly elastic solid. *Journal of Elasticity*, 42, 165-176.

Horgan, C.O. & Murphy, J.G.(2009). Compression tests and constitutive models for the slight compressibilty of elastic rubber-like materials. *International Journal of Engineering Science*, 47, 11-12.

Horgan, C.O. & Murphy, J.G.(2009). Constitutive modeling for moderate deformations of slightly compressible rubber. *Journal of Rheology*, 53(1), 153-168.

Horgan, C.O. & Murphy, J.G.(2010). Simple shearing of incompressible and slightly compressible isotropic nonlinearly elastic materials. *Journal of Elasticity*, 98(2), 205-221.

Horgan, C.O., & Murphy, J.G.(2011). Torsion of incompressible fibre-reinforced nonlinearly elastiv circular cylinders. *Journal of Elasticity*, 103(2), 235-246.

Horgan, C.O., & Murphy, J.G.(2012). Finite extension and torsion of fiber reinforced non-linearly elastic circular cylinders. *International Journal of Non-Linear Mechanics*, 47(2), 97-104.

Horgan, C.O.(2015). The remarkable Gent constitutive model for hyperelastic materials. *International Journal of Non-Linear Mechanics*, 68, 9-16.

Hoss, L., & Marczak, R.J.(2010). A new constitutive model for rubber-like materials. *Mechanica computational*, 29, 2759-2773.

Hossain, M., & Steinman, P.(2012). More hyperelastic models for rubber-like materials: consistent tangent operators and comparative study. *Journal of the Mechanical Behaviour of Materials*, 22(1-2), 27-50.

Huang, Z.(1985). On the Finite Displacement Problem of a Hollow Sphere Under Internal and External Pressures. *Applied Mathematics and Mechanics*, 6, 1097-1102.

Huang, J.L., Xie G.J., & Liu, Z.W.(2008). FEA of hyperelastic rubber material based on Mooney-Rivlin model and Yeoh model[J]. *China Rubber Industry*.

Itskov, M. & Aksel, N.(2004):A Constitutive model for orthotropic elasto-plasticity at large strains. *Archive of Applied Mechanics*, vol.74, 75-91.

Ivanov, T., & Nikolova, E.(2016). Stability analysis of inflation of internally pressurized hyperelastic spherical membranes connected to aneurysm progression. *Institute of Mechanics, Bulgaria Academy of Sciences*, 1-13.

Jianlong, H., Guangjuan, X., & Zhengwei, L.(2008). Finite element analyis of super-elastic rubber materials based on Mooney-Rivlin and Yeoh model. *China Rubber/Plastics Technology and Equipment*, 12, 2176.

Jongmin, S., & Dirk, M.(2011). Rate dependent finite strain constitutive model of polyurea. *International Journal of Plasticity*, 27, 868-886.

Juergen, T.(2005):Financial Engineering with finite elements. *d-fine GmbH Company*, 278.

Kanner, L.M., & Horgan, C.O.(2008). The research by Kanner & Horgan(2008) on extension and torsion of strain-stiffening discussed about the effect on the response of soild circular cylinders in the combined deformation of torsion layered on axial extension. The result of axial force required to maintain pure torsion is compressive for the models considered.. *Journal of Elasticity*, 93(1), 39-61.

Kao, H.P., Steven, R.L., Kendall, H., Kurt, R. Stenmark, R.S. & Jerry, Q.H.(2010):Constitutive modeling of anisotropic finite - deformation of hyperelastic behaviours of soft materials reinforced by tourtous fibre. *International Journal of Structural Changes in Solids:mechanics and applications*, 2(1), 19 - 29.

Khajehasaeid, H., Arghavani, J., & Naghdabadi, R.(2013). A hyperelastic constitutive model for rubber-like materials. *European Journal of Mechanics-A/Solids*, 38, 144-151.

Koprowski-Theib, N., Johlitz, M., & Diebels, S.(2012). Pressure dependent properties of a compressible polymer. *Experimental Mechanics*, 52(3), 257-264.

Kulcu, I.D.(2019). A hyperelastic constitutive model for rubber-like materials. *Archive of Applied Mechanics*, 1-8.

Kumar, N., & Rao, V.V.(2016). Hyperelastic Moony-Rivlin model: Determination and physical interpretation of material constants. *Parameters*, 2(10), 01.

Lev, Y., & Volokh, K.Y.(2016). On cavitation in rubber-like materials. *Journal of Applied Mechanics*, 83(4), 044501.

Levinson, M. & Burgess, I.W.(1971):A Comparison of some simple constitutive relations for

slightly compressible rubber-like materials. *International Journal of Mechanical Sciences*,13, 563-572.

Levyakov, S.V.(2017). The effect of inflating pressure on the finite pure bending of hyperelastic tubes. *ZAMM Journal of Applied Mathematics and Mechanics*, 97(5), 561-575.

Li, X., & Wei, Y.(2015). Classic strain energy functions and constitutive tests for rubber-like materials. *Rubber Chemistry and Technology*, 88(4), 604-627.

Mangan, R., Destrade, M., & Saccommandi, G.(2016). Strain energy function for isotropic nonlinear elastic incompressible solids with linear finite strain response in shear and torsion. *Extreme Mechanics Letters*, 9, 204-206.

Maqueda, L.G., Mohammed, A.N.A., & Shabana, A.A.(2010). Use of general nonlinear material models in beam problems: Application to belts and rubber chains. *Journal of Computational and Nonlinear Dynamics*, 5(2), 021003.

Moalemi, A., Baghani, M., Almasi, A., Zakerzadeh, M.R., & Baniassadi, M.(2018). Large deformation and stability analysis of functionally graded pressure vessels: An analytical and numerical study. *Proceedings of the Institution of Mechanical Engineering Science*, 232(18), 3300-3314.

Moreira, D.C., and Numes, L.C.(2013). Comparison of simple and plane shear for an incompressible isotropic hyperelastic material under large deformation. *Polymer Testing*, 32(2), 240-248.

Muamar, B., Bojan, R., Rabic, A.G., & Zoran, S.(2014):Numerical simulation as a tool for optimizing tool Geometry for rubber pad forming process. *FME Transactions* vol.42, 63-67.

Ogden, R. W.(2001). Non-linear elastic deformations. In R.W. Ogden, Elements of the theory of finite elasticity, Nonlinear elasticity. *Dover edition ed. Cambridge: Cambridge university press*, 1-57.

Ogden, R.W., Chadwick, P. & Haddon, E.W.(1973).Combined axial and torsional shear of a tube of incompressible isotropic elastic material. *The Quarterly Journal of Mechanics and Applied Mathematics*, vol.26, 34-41.

Pascon, J.P., & Coda, H.B.(2013). Large deformation analysis of homogeneous rubber-like materials via shell finite elements. *Latin American Journal of Solids and Structures*, 10(6),

1177-1209.

Pence, T.J., & Gou, K.(2015). On compressible versions of the incompressible neo-Hookean material. *Mathematics and Mechanics of Solids*, 20(2), 157-182.

Peyrant, F., Feng, Z.Q., He, Q.C., & Label, N.(2009). Robust numerical analysis of homogeneous and non-homogeneous deformations. Applied Numerical Mathematics, 59(7), 1499-1514.

Polignone, D.A & Horgan, C. O. ,(1991): Pure torsion of compressible nonlinearly elastic circular cylinders. *Quart. Applied Mathematics*, 49, 591-607.

Pucci, E., & Saccomandi, G.(2013). Secondary motions associated with anti-plane shear in nonlinear isotropic elasticity. *The Quarterly Journal of Mechanics and Applied Mathematics*, 66(2), 221-239.

Puglsi, G., & Saccomandi, G.(2015). The Gent Model for rubber-like materials: an appraisal for an ingenious and simple idea. *International Journal of Non-Linear Mechanics*, 68, 17-24.

Puglisi G. & Saccomandi G. (2016). Multi-scale modelling of rubber-like materials and soft tissues: An appraisal. *Proceedings of Mathematical Physics and Engineering Sciences*, 1-19

Rivlin R.S & Ericksen J.L (1955): Stress-Deformation relations for isotropic materials. *Journal of Rational Mechanics*, 4(2), 911 - 1013.

Rivlin, R.S(1949): Large elastic deformations of isotropic materials v. The problem of flexure. *Journal of the Royal Society*, A195, 463-473.

Sang, J., Xing, S., Liu, H., Li, X., Wang, J., & Lv, Y.(2016). Large deformation analysis and stability analysis of a cylindrical rubber tube under internal pressure. *Journal of Theoritical and Applied Mechanics*, 55(1), 177-188.

Sasso, M., Palmieri, G., Chiappini, G., & Amodio, D.(2008). Characterization of hyperelastic rubber-like materials by biaxial and uniaxial stretching tests based on optical methods. *Polymer Testing*, 27(8), 995-1004.

Shahzad, M., Kamran, A., Siddiqui, M.Z., & Farhan, M.(2015). Mechanical characterization and FE moedling of a hyperelastic material. *Materials Research*, 18(5), 918-924.

Singh, J.(2013): A nonlinear shooting method and its application nonlinear Rayleigh Benard convection. *ISRN Mathematical Physics*, 2013, 1-10.

Stange, J.B.(1984): Finite Deformation of Hollow Sphere of Linear Elastic Perfectly Plastic Material. *Acta Mechanica*, 50, 201-209.

Steinmann, P., Mokarram, H. & Gunnar, P.(2012): Hyperelastic models for rubber-like materials:Consistent tangent operators and suitability for Treolar's data. *Archive of Applied Mechanics*, 82, 1183-1217.

Valiollahi, A., Shojaeifard, M., & Baghani, M.(2019). Closed form solutions for large deformation of cylinders under combined extension-torsion. *International Journal of Mechanical Sciences*, 157, 336-347.

Volokh, K.Y.(2010). On modeling failure of rubber-like materials. *Mechanics Research Communications*, 37(8), 684-689.

Wen, Y., and Zhao, W.(2013). Finite deformation of everted spherical shells composed of incompressible hyperelastic materials. *Applied Mathematical Sciences*, 7(65-68), 3303-3308.

Wriggers, P.(2016). Discretization methods for solids undergoing finite deformations. *In Advanced Finite Technologies, Springer, Cham*, 17-51.

Xiao, H., Yue, Z.F. & He, L.H.(2011). Hill's class of compressible elastic materials and finite bending problems: Exact solutions in unified form. *International Journal of Solids and Structures*, 48(9), 1340-1348.

Yaya, K., & Bechir(2018). A new hyper-elastic model for predicting multi-axial behaviour of rubber-like materials: formulation and computational aspects. *Mechanics of Time-Dependent Materials*, 22(2), 167-186.

Yuan, L., Gu, Z.X., Yin, Z.N., & Xiao, H.(2015). New compressible hyperelastic models for rubber-like materials. *Acta Mechanica*, 226(12), 4059-4072.

Yukeler, R.F.(2015). A theory of rubber-like rods. *International Journal of Solids and Structures*, 69, 350-359.

Zehil, G.P., & Gavin, H.P.(2013). Unified constitutive modeling of rubber-like materials under diverse loading conditions. *International Journal of Engineering*, 62, 90-105.

Zhang, Y.Y., Li, H., & Xiao, H.(2014). Further study of rubber-like elasticity: Elastic potentials matching biaxial data. *Applied Mathematics and Mechanics*, 35(1), 13-24.

Zhao, F.(2016). Continuum constitutive modeling for isotropic hyperelastic materials. *Advances in Pure Mathematics*, 69(09), 571-582.

Zhukov, B.A.(2015). Nonlinear interaction of finite longitudinal shear with finite torsion of a rubber-like bushing. *Mechanics of Solids*, 50(3), 337-344.

The SPERICAL PROBLEM

```
a = 0.2; b = 1; μ = 0.46; ρ = 0.5; (*Initial conditions and parameters*)
```

```
coef1 = 2 r[R]^2 + 25 r[R]^4 R; coef2 = 50 r[R]^3 r'[R]^2 R; coef3 = (4 R^4 - 50 r[R]^4); coef4 = 2 r[R] R^3
(*Coefficients of the dif. eqn.*)
```

$$bc1 = \frac{r[a]^2\, a^2}{\mu}\left(\frac{27\,\mu - 2\,\rho}{2\,a^4 + 25\,r[a]^4}\right);\quad bc2 = \frac{27\,r[b]^2\, b^2}{2\,b^4 + 25\,r[b]^4};$$

```
(*Left and Right Boundary conditions*)
```

```
Eqn = {coef1 r''[R] + coef2 + coef3 r'[R] - coef4 == 0}; (*The main differential Equation*)
```

```
bc = {r'[a] == bc1, r'[b] == bc2}; (*Boundary conditions*)
```

The “Shooting” method algorithm

```
sols = Map[First[NDSolve[{Eqn, bc}, r, R, Method → {"Shooting", "StartingInitialConditions" →
    {1}]];
```

Table of Solutions at different mesh points

```
Table[{R, Evaluate[r[R] /. sols]}, {R, 0.2, 1, 0.02}] // TableForm
```

The CYLINDRICAL PROBLEM

```
a = 0.2; b = 1; μ = 0.46; ρ = 14; gam = 1.0315;(*Initial conditions and parameters*)
```

```
coef1 = 2 R^3 + 25 r[R]^2 R gam^2; coef2 = 25 r[R] gam^2 R; coef3 = -(2 R^2 - 25 r[R]^2 gam^2); coef4 = 2 r[R]
(*Coefficients of the dif. eqn.*);
```

$$bc1 = \frac{r[a]\ gam\ (27 - \rho)}{2\,a^2 + 25\,r[a]^2\ gam^2};\quad bc2 = \frac{27\,r[b]\ b\ gam}{2\,b^2 + 25\,r[b]^2\ gam^2};$$

```
(*Left and Right Boundary conditions*)
```

```
Eqn = {coef1 r''[R] - coef2 r'[R]^2 + coef3 r'[R] - coef4 == 0};(*The main differential Equation*
```

```
bc = {r'[a] == bc1, r'[b] == bc2}; (*Boundary conditions*)
```

The “Shooting” method algorithm

```
sols = Map[First[NDSolve[{Eqn, bc}, r, R, Method → {"Shooting", "StartingInitialConditions" →
    {1}]];
```

Table of Solutions at different mesh points

```
Table[{R, Evaluate[r[R] /. sols]}, {R, 0.2, 1, 0.02}] // TableForm
```

The CYLINDRICAL PROBLEM

```
a = 0.2; b = 1; μ = 0.46; ρ = 14; gam = 1.0315;(*Initial conditions and parameters*)

coef1 = 2 R^3 + 25 r[R]^2 R gam^2; coef2 = 25 r[R] gam^2 R; coef3 = -(2 R^2 - 25 r[R]^2 gam^2); coef4 = 2 r[R
(*Coefficients of the dif. eqn.*);

bc1 = r[a] gam (27 - ρ) / (2 a^2 + 25 r[a]^2 gam^2); bc2 = 27 r[b] b gam / (2 b^2 + 25 r[b]^2 gam^2); (*Left and Right Boundary conditions*)

Eqn = {coef1 r''[R] - coef2 r'[R]^2 + coef3 r'[R] - coef4 == 0};(*The main differential Equation

bc = {r'[a] == bc1, r'[b] == bc2}; (*Boundary conditions*)
```

The “Shooting” method algorithm

```
sols = Map[First[NDSolve[{Eqn, bc}, r, R, Method → {"Shooting", "StartingInitialConditions"
   {1}];
```

Table of Solutions at different mesh points

```
Table[{R, Evaluate[r'[R] /. sols]}, {R, 0.2, 1, 0.02}] // TableForm
```

```
a = 0.2; b = 1; μ = 0.46; ρ = 0.5; (*Initial conditions and parameters*)

coef1 = 2 r[R]^2 + 25 r[R]^4 R; coef2 = 50 r[R]^3 r'[R]^2 R; coef3 = (4 R^4 - 50 r[R]^4); coef4 = 2 r[R] R^3
(*Coefficients of the dif. eqn.*)

bc1 = r[a]^2 a^2 / μ (27 μ - 2 ρ) / (2 a^4 + 25 r[a]^4); bc2 = 27 r[b]^2 b^2 / (2 b^4 + 25 r[b]^4); (*Left and Right Boundary conditions*)

Eqn = {coef1 r''[R] + coef2 + coef3 r'[R] - coef4 == 0}; (*The main differential Equation*)

bc = {r'[a] == bc1, r'[b] == bc2}; (*Boundary conditions*)
```

The “Shooting” method algorithm

```
sols = Map[First[NDSolve[{Eqn, bc}, r, R, Method → {"Shooting", "StartingInitialConditions"
   {1}];
```

Table of Solutions at different mesh points

```
Table[{R, Evaluate[r'[R] /. sols]}, {R, 0.2, 1, 0.02}] // TableForm
```

code for calculating the cylindrical stresses

$a = 1.00;$

$b = 1\ ;$

$\mu = 0.46;$

$\rho = 14;$

$\gamma = 1.0315;$

$x_a = 1.16626;$

$r_a = 0.85065;$

$t_a = (\frac{\mu}{2}) * \frac{((2*ra*a)}{(xa*(\gamma))+(25*ra*xa*(\gamma))/a-27)};$

$disp(t_a)$

code for calculating the spherical stresses

$a = 1.00;$

$\mu = 0.46;$

$x_a = 0.03705;$

$r_a = 0.01853;$

$t_a = (\frac{\mu}{2})(\frac{((2*ra*a^2)}{xa^2+(25*ra*xa^2)/a^2-27)})$

$disp(t_a)$